IDENTIFICATION OF TROPONIN C RESIDUES THAT INCREASE MAMMALIAN CARDIAC MYOCYTE CONTRACTILITY

by

Franca Wing Ping Chung
BSc (Biochemistry) University of British Columbia 2002

THESIS SUBMITTED IN PARTIAL FULFILLMENT OF
THE REQUIREMENTS FOR THE DEGREE OF

MASTER OF SCIENCE

In the
School
of
Kinesiology

SIMON FRASER UNIVERSITY

Summer 2006

APPROVAL

Name: **Franca Wing Ping Chung**

Degree: Master of Science

Title of Thesis: Identification of Troponin C Residues that Increase Mammalian Cardiac Myocyte Contractility

Examining Committee:

Chair: **Dr. Ted Milner**
Professor

Dr. Glen Tibbits
Senior Supervisor
Professor, School of Kinesiology

Dr. Eric Accili
Supervisor
Professor, Dept. of Cell & Physiol Sciences, UBC

Dr. Wade Parkhouse
External Examiner
Professor, School of Kinesiology

Date Defended/Approved: 29th May 2006

SIMON FRASER UNIVERSITY library

STATEMENT OF ETHICS APPROVAL

The author, whose name appears on the title page of this work, has obtained, for the research described in this work, either:

(a) Human research ethics approval from the Simon Fraser University Office of Research Ethics,

or

(b) Advance approval of the animal care protocol from the University Animal Care Committee of Simon Fraser University;

or has conducted the research

(c) as a co-investigator, in a research project approved in advance,

or

(d) as a member of a course approved in advance for minimal risk human research, by the Office of Research Ethics.

A copy of the approval letter has been filed at the Theses Office of the University Library at the time of submission of this thesis or project.

The original application for approval and letter of approval are filed with the relevant offices. Inquiries may be directed to those authorities.

Bennett Library
Simon Fraser University
Burnaby, BC, Canada

ABSTRACT

Cardiac troponin C (cTnC) is a highly conserved Ca^{2+} binding protein that plays an essential role in cardiomyocyte contraction. Sequence differences between cTnC homologs have been shown to be responsible for differential Ca^{2+} sensitivity. A series of substitutions (D2N, V28I, L29Q and G30D) in salmonid cTnC (ScTnC) accounts for a two-fold higher Ca^{2+} affinity and sensitivity compared to mammalian cTnC (McTnC). The single L29Q substitution that is associated with familial hypertrophic cardiomyopathy (FHC) shows an approximately 35% increase in Ca^{2+} affinity and sensitivity. A skeletal-cardiac TnC chimeric construct confirms the N-terminal domain role as the main determinant of Ca^{2+} affinity and sensitivity. Increasing contractility through modification of Ca^{2+} sensitivity presents a novel means of treating a failing heart and thus the overall objective of this thesis is to provide further insights into cTnC structure and function which can be used in rational drug design for the treatment of heart failure.

Keywords:

Troponin C;
Ca^{2+} binding properties;
Ca^{2+} sensitivity;
Single cardiomyocyte preparation;
7-azatryptophan.

ACKNOWLEDGEMENTS

I would like to thank my supervisor Dr. Glen Tibbits for his trust in me for allowing me to pursue graduate work. I have become a better scientist under his guidance and tutorage. I would also like to thank Dr. Eric Accili for his encouragement and time and Dr. Wade Parkhouse for validating my work as my external examiner.

I also owe many thanks to the past and present members of the Tibbits lab and those who have provided me with guidance and support over my years of academic training at Simon Fraser University. I am very grateful to Dr. Todd Gillis, Dr. Christian Marshall, and Bo Liang who have helped and taught me everything from basic lab techniques to good English writing. I would like to thank Dr. Michael Regnier of the University of Washington for the use of his spectrofluorometer and his generous gift of rabbit skeletal troponin C in pET vector; Dr. Chuck Farah of the Universidade de São Paulo for his kind gift of the CY(DE3)pLysS cells; Dr. Michel Leroux of Simon Fraser University and his lab for the use of his HPLC machine; Dr. Jonathan Davis of the Ohio State University and his group for measuring the binding kinetics of troponin C in this study. It was a privilege and honour to have worked with such fine investigators and collaborators.

Finally, I would like to thank my wonderful family and friends for their continued love and appreciation. They have enriched my life in ways I cannot imagine. Their encouragements, strengths, and wisdom have inspired me to be the best I can be. Thank you.

TABLE OF CONTENTS

LIST OF FIGURES

LIST OF TABLES

LIST OF ABBREVIATIONS

5HW	5-hydroxyltryptophan
7ZW	7-azatryptophan
ACTs	Artificial Ca^{2+} Transients
ANOVA	Analysis of Variance between groups
BcTnC	Bovine cTnC
CHF	Congestive Heart Failure
Chimeric TnC	N-terminus Rabbit Skeletal TnC (residues 1-87) and C-terminus Bovine Cardiac TnC (residues 88-160)
CICR	Calcium Induced Calcium Release
cTnC	Cardiac TnC
cTnI	Cardiac TnI
cTnT	Cardiac TnT
DHPR	Dihydropyridine receptors
DVLG ScTnC	ScTnC with asparagine 2 replaced with aspartate; isoleucine 28 replaced with valine; glutamine 29 replaced with leucine; aspartate 30 replaced with glycine
ECC	Excitation-Contraction Coupling
F	Ca^{2+}-activated force
F27W	Phenylalanine 27 replaced with tryptophan
F27ZW	Phenylalanine 27 replaced with 7-azatryptophan
FHC	Familial Hypertrophic Cardiomyopathy
F_{max}	Maximal Ca^{2+}-activated force
HcTnC	Human cTnC
IPTG	Isopropyl-1-thio-β-D-galactoside
IQD McNTnC	N-terminus (residues 1-89) of McTnC with valine 28 replaced with isoleucine, leucine 29 replaced with glutamine, and glycine 30 replaced with aspartate
IQD McTnC	McTnC with valine 28 replaced with isoleucine, leucine 29 replaced with glutamine, and glycine 30 replaced with aspartate

K_A	Association constant
K_d	Dissociation constant
$K_{f1/2}$	pCa at half-maximal fluorescence
$K_{F1/2}$	pCa at half-maximal force
k_{off}	Dissociation rate constant
k_{on}	Association rate constant
L29Q McTnC	McTnC with leucine 29 replaced with glutamine
LB	Luria-Bertani
MALDI-TOF MS	Matrix Assisted Laser Desorption/Ionization-Time-of-flight Mass Spectrometry
MBP-2	Myosin Binding Protein-C
McNTnC	N-terminus (residues 1-89) of McTnC
McTnC	Mammalian cTnC also know as bovine/human/porcine cTnC
mcTnC	Endogenous pre-extracted mouse cTnC
NIQD McNTnC	N-terminus (residues 1-89) of McTnC with aspirate 2 replaced with asparagines, valine 28 replaced with isoleucine, leucine 29 replaced with glutamine, and glycine 30 replaced with aspartate
NIQD McTnC	McTnC with aspirate 2 replaced with asparagines, valine 28 replaced with isoleucine, leucine 29 replaced with glutamine, and glycine 30 replaced with aspartate
P_i	Inorganic phosphate
RsTnC	Rabbit skeletal TnC
RyR	Ryanodine Receptor
ScNTnC	N-terminus (residues 1-89) of ScTnC
ScTnC	Salmonid cardiac TnC
SERCA	Sarco-Endoplasmic Reticulum Calcium ATPase
SR	Sarcoplasmic Reticulum
sTnC	Skeletal TnC
sTnI	Skeletal TnI
TnC	Troponin C
TnI	Troponin I
TnT	Troponin T
T-tubules	Transverse Tubules

1. GENERAL INTRODUCTION AND LITERATURE REVIEW

1.1 Introduction

Calcium (Ca^{2+}) is an important signalling molecule used in virtually all cell types. In striated muscle, the binding of Ca^{2+} to troponin C (TnC) triggers a cascade of events that ultimately leads to cell shortening and force generation. TnC is conserved across a phylogenetically diverse group of organisms where differential Ca^{2+} affinities of TnC homologs play an important role in regulating contractility (*1, 2*). In order to further explore the contribution of amino acid sequence to TnC Ca^{2+} sensitivity, two complimentary experimental approaches were employed. The first approach examines the protein *in vitro*, and uses steady state spectrofluorometry in conjunction with stopped-flow analysis to obtain data on the K_d (dissociation constant), k_{on} (association rate constant), and k_{off} (dissociation rate constant) of Ca^{2+} binding to various TnC mutants with altered Ca^{2+} affinity. The second approach involves examination of TnC *in situ* and how these substitutions may effect its interaction with other proteins including TnI and TnT.

The overall purpose of this thesis is to identify all the residues responsible for the relatively high Ca^{2+} affinity of full length ScTnC and to determine the efficacy of 7-azatryptophan use *in situ*. A better understanding of the structure function relationship of the cTnC molecule should provide important data for the rational design of future Ca^{2+} sensitizing agents for the treatment of heart failure.

1.2 Excitation-Contraction Coupling (ECC) in the adult heart

Excitation-Contraction Coupling (ECC) (Figure 1-1) involves the mechanisms by which electrical excitation leads to cross-bridge activity in muscle fibres. In the heart, the plasma-membrane action potential is spread as a depolarization wave along the surface and down the transverse tubules (T-tubules) that protrude into the cell. In the adult mammalian heart, depolarization opens voltage-sensitive L-type Ca^{2+} channels, also known as dihydropyridine receptors (DHPR), located in the sarcolemma leading to a small increase in cytosolic Ca^{2+} concentration (a maximum of 10–20 μmol/kg wet weight Ca^{2+}) (*3*). For a normal contraction (30 to 70% maximal force) to occur in a adult rat heart, 30 to 50 μmol/kg wet weight Ca^{2+} is required to enter into the cytosol (*4*). This relatively small increase in cytosolic Ca^{2+} concentration in turn leads to a greater Ca^{2+} release from the sarcoplasmic reticulum (SR) through the activation of the SR Ca^{2+} release channel (or ryanodine receptor – RyR) and is termed "calcium-induced calcium release" (CICR). The combined Ca^{2+} influx and release from the SR increases free cytosolic Ca^{2+}concentration several fold allowing for Ca^{2+} binding to TnC which initiates contractile reaction. The end result is ATP hydrolysis by myosin ATPase transforming chemical energy into mechanical cell shortening.

Figure 1-1. Cardiac excitation-contraction coupling inside a ventricular myocyte.

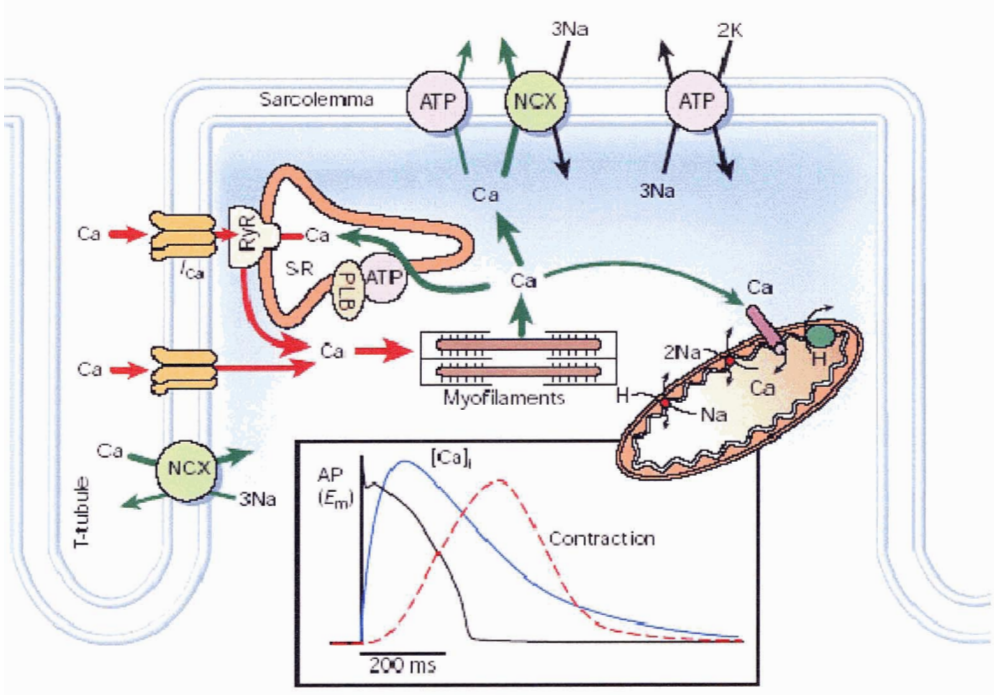

Adapted by permission from Macmillan Publishers Ltd: "Cardiac excitation-contraction coupling" (*5*), Copyright 2002. www.nature.com

Relaxation of the myocyte occurs when the cytosolic Ca^{2+} level is returned to its original low value (~100 nM) by active transport of Ca^{2+}out of the cytosol and Ca^{2+} reuptake by the SR resulting in Ca^{2+} dissociation from TnC. The major route (~ 70%) of cytosolic Ca^{2+} removal is reuptake into the SR by the ATP-dependent pump SERCA (sarco-endoplasmic reticulum calcium ATPase). The secondary route (~ 30%) is through the Na^{+}/Ca^{2+} exchanger, an active transporter located on the sarcolemma. A small amount of Ca^{2+} is removed of the cytosol by the sarcolemmal Ca^{2+}-ATPase and mitochondrial Ca^{2+} uniport system. Overall, there is no net change in the SR Ca^{2+} concentration on a beat to beat basis and the amount of Ca^{2+} that enters the cell to trigger CICR is roughly equivalent to that removed by the Na^{+}/Ca^{2+} exchanger.

1.3 Myofilament structure and function

Well organized striated myofilaments occupying 45 to 60% of the cell volume can be found in close proximity to the SR in the cardiomyocyte. The cross-striations of the cardiac muscle reveal the organization of the contractile proteins into thin (actin) and thick (myosin) filaments. Each sarcomere is bounded by Z-lines, which serve as an anchoring point where the intermediate filaments attach the thin filament to the sarcomere. The thin filament is mainly composed of two intertwined helical chains of G-actin molecules forming the F-actin polymer which is approximately 1 μm long and 10 nm thick (*4*). Aligned with the actin backbone is the rod shaped tropomyosin molecule which is ~ 42 nm long (*6*). Tropomyosin plays a critical role in the dynamics of actin filament and in muscle and non-muscle function. The primary role of tropomyosin is to regulate the interaction of thin and thick filaments in conjunction with troponin complex. One troponin complex, consisting of TnC, TnI, and TnT is associated with each tropomyosin molecule and each tropomyosin molecule stretches along 7 actin molecules (Figure 1-2). The structure and function of the troponin complex will be discussed in greater detail in the next section.

Figure 1-2. **A molecular model of the troponin complex on the thin filament. The troponin complex (orange TnC, green TnI, and yellow TnT) are shown as they lie along the double stranded tropomyosin.**

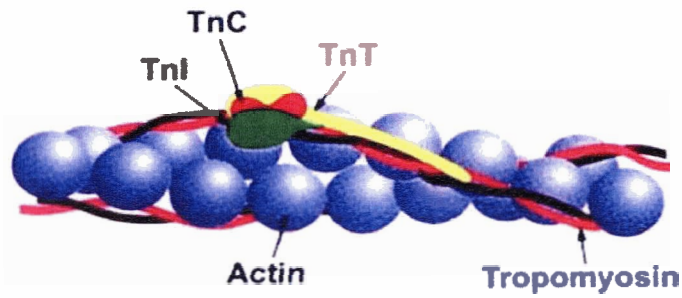

Adapted by permission from the American Physiological Society: "Skeletal and cardiac muscle contractile activation: tropomyosin 'rocks and rolls'" (*7*), Copyright 2001.

The thick filament is a bipolar polymer mainly composed of ~ 300 myosin molecules and other proteins such as titin and myosin binding protein-C (MBP-2) (*4*). The myosin filaments are ~ 1.6 μm long and ~ 15 nm thick and each myosin molecule is ~ 170 nm in length consisting of one pair of myosin heavy chains and two pairs of myosin light chains (*4*). The myosin heavy chains wrap around each other to form a double helix and are subdivided into light meromyosin and heavy meromyosin. The light meromyosin is thinner and longer (~ 100 nm) while the heavy meromyosin is shorter and more globular. The heavy meromyosin itself is further divided into S1 (~ 20 nm) and S2 (~ 50 nm) subunits. The S1 fragment is know as the "head" and the S2 fragment is known as the "arm". It is in the S1 fragment (myosin head) that ATP hydrolysis and cross-bridge formation take place. The S2 fragment and the light meromyosin together make up the myosin "tail". The myosin light chains are divided into MLC1 and MLC 2 and bind to the base of the myosin head S1. Both light chains are thought to provide physical stability.

The myosin tails aggregate in a very specific manner to form the central axis of the thick filament. The myosin heads project from the thick filament in pairs separated by 180°. Adjacent myosin heads are located 14.3 nm and rotated 60° relative to each other creating a helical arrangement of heads. Within each row, the cross bridges are separated by 42.9 nm. The myosin heads are always oriented toward the end of the thick filament creating a ~ 200 nm central bare zone on either side of the M lines that contains only tails and no heads (Figure 1-3). The two adjacent bare zones (~ 400 nm) are encompassed within the H-band where there is no thin filament. The M line acts to maintain the stability of the thin and thick filament matrix. The thick filament is further stabilized within the sarcomere by titin with one end attached to the Z-line and the other to the M-line. Titin is a vast, modular protein containing an elastic element that acts as a molecular spring to help to maintain sarcomeric elasticity. It also plays a role in muscle elasticity and the generation of passive tension (*8*). The A-band and I-band are named after their properties under a polarized microscope. The anisotropic A-band, containing both thin and thick filaments is located in the middle of the sarcomere. The isotropy I-band is located on the end of one sarcomere and the beginning of the next sarcomere. It contains only the thin filament and is bisected by the Z-line.

Figure 1-3. Schematic of the cardiac sarcomere.

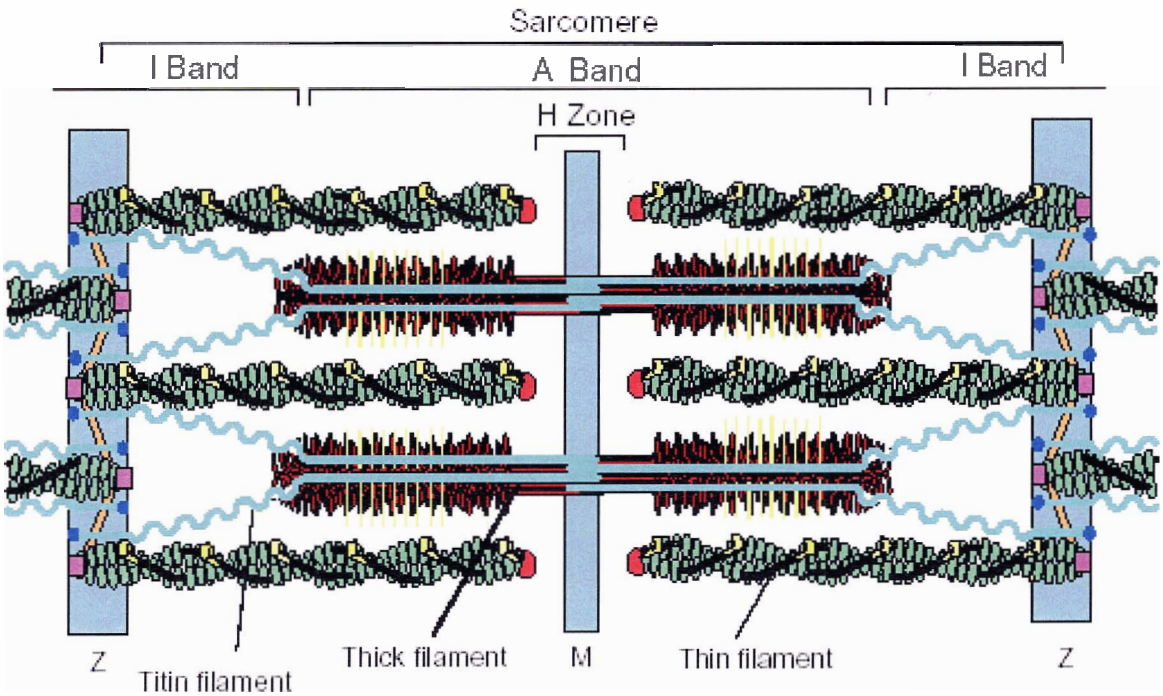

Reprinted from "To the heart of myofibril assembly" (*9*), Copyright 2000, with permission from Elsevier.

1.4 The troponin complex: TnC, TnI, and TnT

Tn is a heteromeric protein complex that plays an important role in the Ca^{2+} induced conformational changes that initiate muscle contraction. It is composed of three interacting subunits of various molecular weights: TnC (~ 18,400 Da), TnI (~ 23,500 Da), and TnT (~ 38,000 Da) (*10*).

TnI is the inhibitory subunit of the troponin complex that completely inhibits *in vitro* actomyosin ATPase activity (*11*). Three TnI paralogs are expressed in the vertebrate genome: a cardiac TnI (cTnI), a fast twitch skeletal TnI (sTnI fast), and a slow twitch skeletal TnI (sTnI slow). The human cTnI consists of 209 amino acids and possess an additional 27 to 33 residue N-terminus tail that is absent in the sTnI fast (181 residues) and sTnI slow (186 residues) isoforms (*12*). It is well established that the binding of TnI with actin and tropomyosin filaments can inhibit Mg^{2+}-dependent actomyosin ATPase activity and that the formation of a 1:1 complex with TnC can neutralize the inhibitory interaction of TnI (*13*). TnI also functions to holds the troponin complex together and binds to actin by a Ca^{2+}-mediated interaction. TnI has thus been termed the "molecular key" of the troponin complex.

TnT is a highly symmetric molecule that can easily be separated into the N-terminus and C-terminus fragment by treating it with chymotrypsin, a protease that catalyzes the hydrolysis of ester bonds. The N-terminus of TnT lies along the C-terminus of tropomyosin including the region of overlap with the neighbouring N-terminus of tropomyosin, whereas C-terminus TnT interacts with TnC, TnI, and tropomyosin (*6*). TnT is expressed in three isoforms in vertebrate species: the cardiac TnT (cTnT), the fast twitch skeletal TnT (sTnT fast), and the slow twitch skeletal TnT (sTnT slow). The

length of TnT varies greatly from 160 to 300 amino acids depending on the species and isoforms. TnT acts to attach the Tn-tropomyosin-actin complex together; thus, it also plays any essential role in Ca^{2+} regulation and in the cooperation of thin filament activation (*6*). However, TnT itself does not significantly affect the inhibitory action of TnI or the contractile interaction the myosin-actin-tropomyosin (*14*).

Figure 1-4. **Sequences alignment of RsTnC and McTnC.**
Rabbit skeletal TnC (RsTnC) (Swiss-Prot accession number P02586) and mammalian cardiac TnC (McTnC) (Swiss-Prot accession number P63315). The differences are shown in bold print (64.6% identical).

```
RsTnC:   1  MTDQQAEARSYLSEEMIAEFKAAFDMFDAD  30
McTnC:   1  -D-IYKA-VEQ-T--QKN-------I-VLG  30

RsTnC:  31 G-GGDISVKELGTVMRMLGQTPTKEELDAI  59
McTnC:  31 AED-C--T------------N------QEM  60

RsTnC:  60 IEEVDEDGSGTIDFEEFLVMMVRQMKED  86
McTnC:  61 -D---------V-D---------C--D-  87

RsTnC:  87 AKGKSEEELAECFRIFDRNADGYIDAEELAEIFRAS  123
McTnC:  88 S--------SDL--M----------L---KIMLQAT  124

RsTnC: 124 GEHVTDEEIESLMKDGDKNNDGRIDFDEFLKMMEGVQ  160
McTnC: 125 --TI-EDD-E---------------Y----EF-K--E  161
```

The genomes of vertebrate species express two TnC paralogs: a slow cardiac/skeletal muscle TnC (cTnC) with relatively low Ca^{2+} affinity and a fast skeletal muscle TnC (sTnC) with a higher Ca^{2+} affinity (*15*). The isoforms vary slightly in residue length with cTnC and sTnC consisting of 161 and 160 residues, respectively. The two isoforms are ~ 65% identical with 54 residue differences (Figure 1-4).

Structurally the TnC isoforms have a similar dumbbell-shape with two globular domains; the N- and C-terminus, separated by a long, flexible α-helix (*16*). Each terminus contains a core of hydrophobic residues that is "closed" in the apo state with majority of the hydrophobic residues buried. Upon Ca^{2+} binding, these hydrophobic cores adopt a more "opened" conformation and expose the previously hidden hydrophobic areas. This hydrophobic patch strengthens the interaction between TnC and TnI thereby pulling TnI away from actin. It is the TnI and actin-tropomyosin complex interaction which inhibits cross-bridge formation. The hydrophobic cores are also important in maintaining the stability of the troponin complex and in the transmission of Ca^{2+} binding signals.

The N- and C- terminus of TnC contains two EF helix-loop-helix Ca^{2+} binding sites. The EF-hand loops are found between helixes A and B (site I), C and D (site II), E and F (site III), and G and H (site IV) (Figure 1-5). Sites I and II are located in the N-terminal domain and sites III and IV in the C- terminus. Sites III and IV are non-specific divalent ion binding sites that possess a several fold higher Ca^{2+} affinity and much slower Ca^{2+} exchange rates compared to sites I and II and are therefore constantly occupied by either Ca^{2+} or Mg^{2+} under resting physiological conditions (*6*).

Figure 1-5. **Ribbon representation of Ca^{2+} bound RsTnC.**
The solid black circles represent Ca^{2+}. The lettered helices are coloured to show orientation.

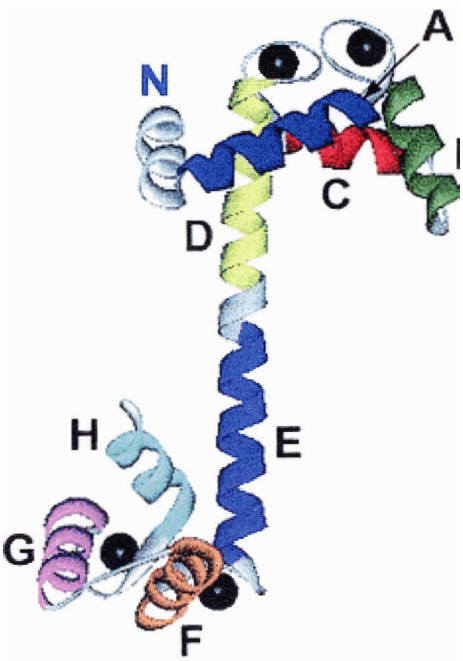

Adapted by permission from the American Physiological Society: "Regulation of contraction in striated muscle" (*6*), Copyright 2000.

The C-terminus is often referred to as the structural domain since the constant presence of Ca^{2+} or Mg^{2+} maintains the integrity of the troponin molecule and prevents TnC dissociation from TnI and the myofibrils (*17*). The N-terminus is known as the regulatory domain as Ca^{2+} binding leads to myocyte contraction while the unbound state results in relaxation. However, the N-terminus differs between TnC paralogs in that both sites I and II bind Ca^{2+} in sTnC whereas site I is inactive in cTnC and does not bind Ca^{2+} (*6*). Site I of cTnC is rendered non-functional due to a single valine insertion at residue 28 and two chelating residue substitutions, aspartate with leucine at residue 29 and aspartate with alanine at residue 31 (*18*). The lack of a functional site I gives cTnC 8-fold lower Ca^{2+} affinity (*19*) and a lower Hill coefficient (*2*) compared to sTnC. In addition, purified cTnC produces only ~ 70% of the maximal Ca^{2+}-activated force when reconstituted into a sTnC skinned fibre (*20, 21*). However, cardiac muscle is ~ 5X more sensitive to activation by Ca^{2+} in skinned fibre compared to skeletal muscle (*22*).

Ca^{2+} binds to the EF-hand helix-loop-helix of TnC through a 12 residue signature sequence with a X, Y, Z, -Y, -X, -Z motif that participates in metal coordination (*23*). The six charged coordinating residues are at positions 1, 3, 5, 7, 9, and 12 in the 12 residue loop with residue 12 acting as the bi-dentate coordination through both side-chain carboxylate oxygens (Figure 1-6) (*24*). The Ca^{2+} ion binds to these six residues forming a pentagonal bi-pyramid pattern.

Figure 1-6. EF-hand Ca^{2+} coordination of N-terminus cTnC.

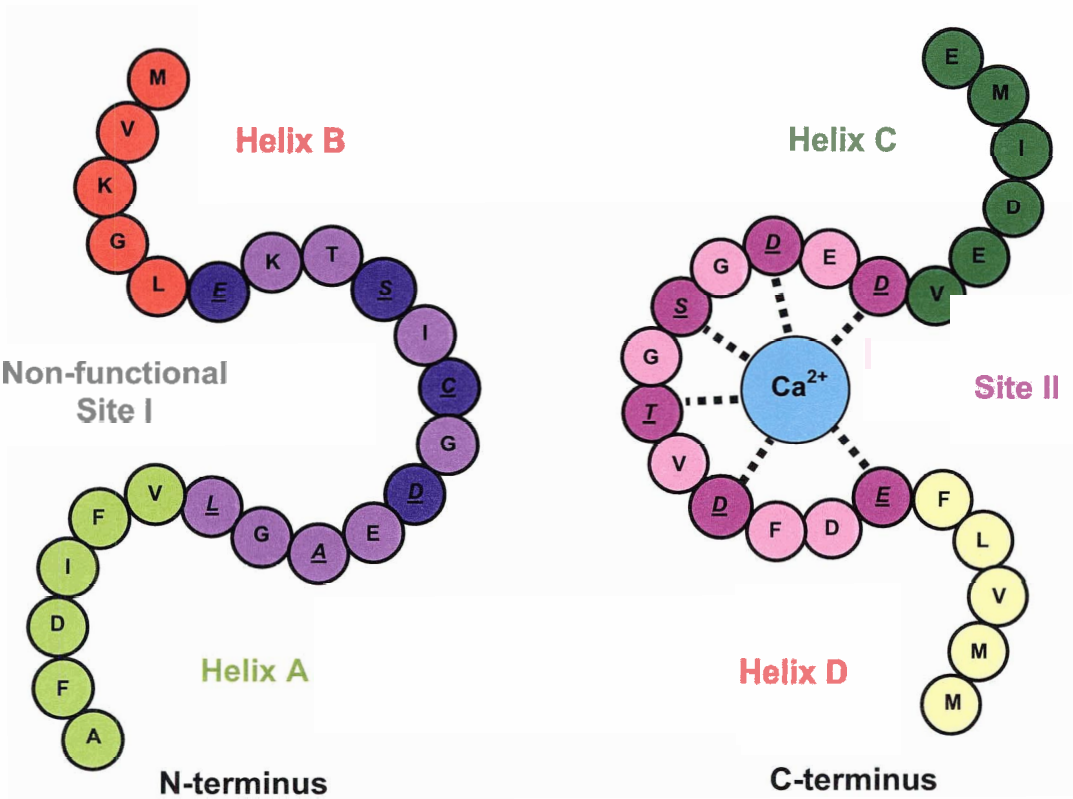

1.5 Contractility and cross-bridge cycling in the heart

Activation of cardiomyocyte contraction by Ca^{2+} is a multi-step complex reaction involving many conformational changes within the thin filaments. During diastole, only the C-terminus of cTnC is occupied by Ca^{2+} or Mg^{2+} with an association constant (K_A) of $\sim 3.7 \times 10^8\ M^{-1}$ and $\sim 3.0 \times 10^3\ M^{-1}$ for Ca^{2+} and Mg^{2+}, respectively under physiological conditions (*4*). The near N-terminus of cardiac TnI (cTnI) (residues 34-71 and 80-136) is bound to the C-terminus of both cTnC and cardiac TnT (cTnT) (*12*). A section of the cTnI (residues 128-147), termed the inhibitory peptide is bound to the actin-tropomyosin complex and inhibits the force generating reaction between actin and myosin (*12*). At the onset of systole, Ca^{2+} is bound to the single activation site (site II) of cTnC and the conformation of the molecule is altered. In the presence of the switch or triggering region of cTnI (residues 147-163), cTnC "opens" as helix B moves away from helix A exposing a 178 $Å^2$ hydrophobic patch (*25*). The hydrophobic patch strengthens cTnC and cTnI interaction as the inhibitory peptide of cTnI switches from the actin-tropomyosin complex to bind to the C-terminus of cTnC. The switching of the cTnI molecule releases its inhibitory effect on actin and myosin heads allowing for cross-bridge formation (Figure 1-7).

Figure 1-7. **The effects of Ca^{2+} binding to cardiac TnC.**
A is actin, Tm is tropomyosin indicated with the head-to-tail overlap of the N-terminus and C-terminus. Thicker lines indicate stronger binding and weaker lines indicate weaker binding. Ca^{2+} binding strengthens TnC-TnI, TnC-TnT, TnT-Tm binding and abolishes TnI-actin binding.

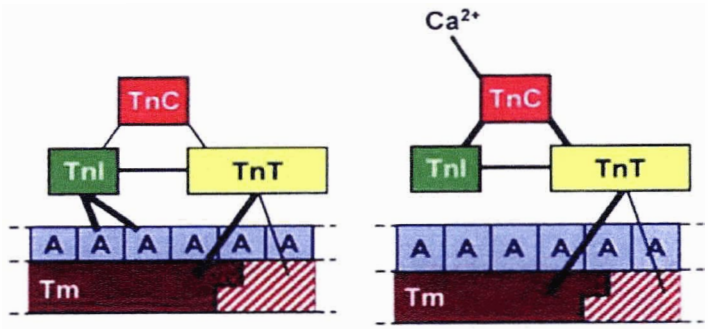

Adapted by permission from the American Physiological Society: "Skeletal and cardiac muscle contractile activation: tropomyosin 'rocks and rolls'" (7), Copyright 2001.

The cross bridge cycle describes the mechanism of actin and myosin interaction where chemical energy of ATP is hydrolysed into mechanical energy. The cross bridge cycle can be described in five steps. In the first step, the myosin in an energized form bound to AD and inorganic phosphate (P_i) at the ATPase site. In presence of Ca^{2+}, the myosin head binds to the adjacent actin on the thin filament. In step 2, ADP and P_i are released to provide energy for the power stroke of muscle contraction. In step 3, the low energy myosin is tightly bound to actin causing a rigor state. In step 4, a new ATP binds to myosin causing conformational changes for cross bridge dissociation. In the last step, the ATP bound to myosin is hydrolysed into ADP and P_i bringing the cycle back to step 1.

1.6 Factors that affect Ca^{2+} sensitivity

Cardiac contractility is heavily dependent on the Ca^{2+} sensitivity of the contractile element, which is modulated by caffeine, pH, temperature, sarcomere length, and the interaction between TnC and TnI (as a result of TnI phosphorylation, hence any β adrenergic agonist). Despite its importance, the molecular mechanism of myofilament Ca^{2+} sensitivity and regulation is poorly understood. This thesis will focus on two of these variables: sarcomere length and the interaction between TnC and TnI.

The relationship between sarcomere length and maximum force generation was first described in detail by Gordon et al (*26*) in a frog skeletal muscle model. The theory postulates that the tension force generated is determined by the number of thin and thick filament overlap (number of cross bridge) (Figure 1-8). The amount of force generated increases with sarcomere length from ~ 1.2-2.2 μm. After the optimal sarcomere length of 2.0-2.2 μm, the force generated decreases with increasing sarcomere length up to 3.6 μm. At sarcomere lengths shorter than 2.0 μm, the thin filaments cross over and hinder effective cross-bridge formation. At sarcomere lengths of 2.0-2.2 μm, the maximum number of cross-bridge is formed between actin and myosin resulting in the maximum force. No force is generated at sarcomere length greater than 3.6 μm because there is no overlap between the thin and thick filaments.

Sarcomere length has a vital effect on the Ca^{2+} sensitivity of myocyte. Increases in sarcomere length within the physiological range (2.0-2.2 μm) result in increased Ca^{2+} affinity (*27*) and Ca^{2+} sensitivity (*28-30*) and is thought to be an important component of mechanism of the Frank-Starling relationship. This length dependent increase is observed in both cardiac and skeletal myocyte but is generally thought to be at least two

times greater in cardiac muscles (*30*). However, these results are contradicted by Moss et al (*39*), who found that the reconstitution of cTnC for sTnC did not alter the length dependence of Ca^{2+} in skinned rabbit psoas muscle. Moss' group proposed that alteration of Ca^{2+} sensitivity in the myocyte is not dependent of the TnC isoform, but instead is due to changes in lattice spacing (*29, 31*). In 2002, de Tombe et al (*32*) rebutted this hypothesis by observing an unaltered Ca^{2+} sensitivity in skinned myocardium under reduced lattice spacing. However, de Tombe's group showed that increases in sarcomere length only increases the Ca^{2+} responsiveness of the cardiac sarcomere but not the level of cooperativity (*33*). The exact mechanism of sarcomere length on Ca^{2+} sensitivity still remains controversial to date.

The second modulator of Ca^{2+} sensitivity discussed here is protein interactions with the troponin complex. Multiple components are involved in cross-bridge cycling and single residue variation in TnI has been shown to have a remarkable affect on Ca^{2+} sensitivity in single fibre (*34*) and *in vitro* (*35*). It is known that the affinity of TnI to actin and other components of the troponin complex vary substantially under different Ca^{2+} binding conditions (*6, 35, 36*) and that the Ca^{2+} affinity of TnC is also affected by the binding of TnC to the inhibitory region of TnI in the presence of Ca^{2+} (*35, 37, 38*). The phosphorylation of TnI also has a profound allosteric effect on TnC's ability to bind Ca^{2+} (*39*). These make TnI an important modulator in the Ca^{2+} affinity of TnC and in cross-bridge cycling.

Figure 1-8. The length-tension relation as described by Gordon et al.

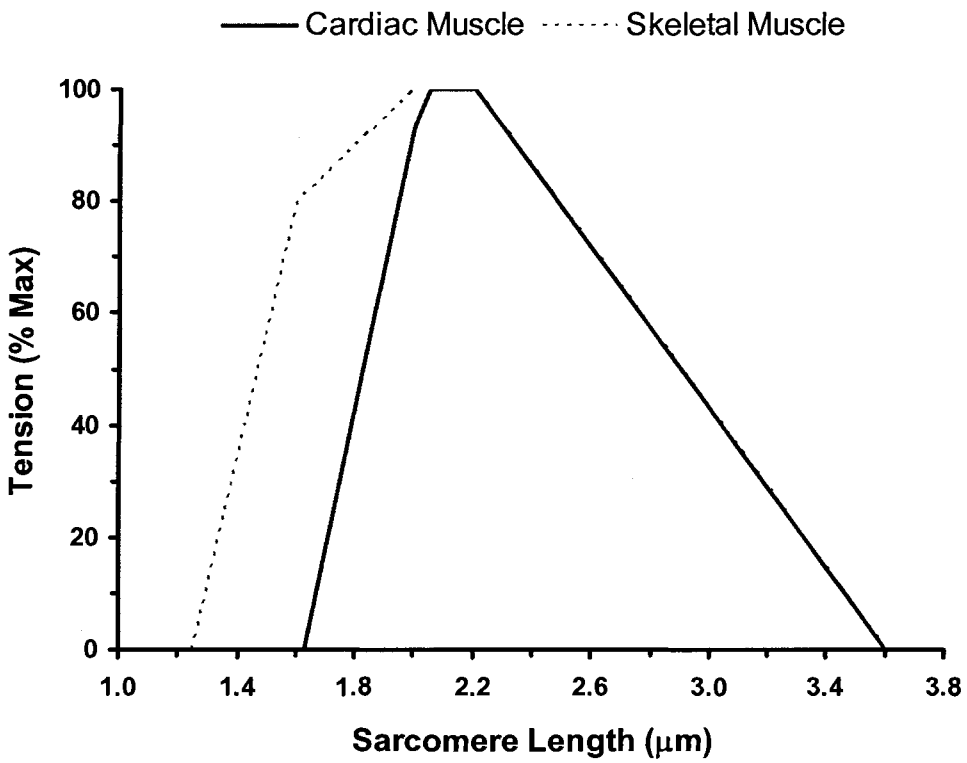

Data source: (*26*).

1.7 Positive inotropic agents: Ca^{2+} sensitizer

Congestive heart failure (CHF) is a common, yet complex cardiovascular disorder where the heart's function as a pump is inadequate to meet the body's needs. This condition is in part characterized by excessive filling pressures, insufficient cardiac output, and decreased cardiac output reserve due to depressed Ca^{2+} contractility and Ca^{2+} desensitization of the myocardium. Due to the increasing occurrence of CHF, there is an immense interest in pharmacological therapy in the search of a positive inotropic agent. Clinically available cardiotonic agents, such as digitalis, β-adrenoreceptor agonists, and selective phosphodiesterase III inhibitors work by increasing the intracellular Ca^{2+} movement (*40*). This increase in cytosolic Ca^{2+} concentration, although beneficial in the short term, may ultimately lead to myocardial cell death due to arrhythmias, myocardial cell injury, and premature cell death as a result of intracellular Ca^{2+} overload (*41*). Ca^{2+} mobilizers are also energetically disadvantageous because they require additional activation energy for the increased Ca^{2+} transients. To date, the use of Ca^{2+} mobilizers have shown little success in reducing the morbidity and mortality rate of patients with CHF (*42*).

Current interests for the treatment of CHF have been placed on another class of pharmacological agents called Ca^{2+} sensitizers, which do not incur the risks of Ca^{2+} mobilizers. Ca^{2+} sensitizers are positive inotropic agents that act by increasing the Ca^{2+} sensitivity of the contractile element without increasing intracellular Ca^{2+}. This is achieved by increasing the Ca^{2+} binding affinity to cTnC, or assisting the process following Ca^{2+} binding to cTnC (*43*). These agents have been found to be effective in reversing the contractile dysfunction in CHF due to little or no effect on Ca^{2+} transients

and heart rate (*40*). Bepridil, Levosimendan, and EMD 57033 are a few of the Ca^{2+} sensitizers that serve to illustrate the important concepts related to Ca^{2+} sensitization and the vital Ca^{2+} signalling protein cTnC (*44*). An understanding of the molecular mechanism of these existing Ca^{2+} sensitizers provides insights into structure function relation of cTnC. These structural data can lead to the rational design of drugs useful in the treatment of heart failures.

1.8 Sequence comparison of mammalian and salmonid cardiac TnC

There exists a high degree of sequence identity at the amino acid level in cTnC isoforms from mammals and salmonids; however, previous spectrofluorometry studies in our lab using truncated salmonid cTnC (ScTnC) (residues 1-89) showed ~ twice the Ca^{2+} affinity when compared to mammalian cTnC (McTnC) (*1*). This increased Ca^{2+}sensitivity of ScTnC is one compensatory mechanism believed to have adapted in ectothermic species to overcome slower binding kinetics at lower temperatures. This increased affinity is thought to allow the trout to maintain cardiac function at physiological temperatures (5-15 °C) that are cardioplegic to mammals.

There are only 13 differences out of the 161 amino acids of the two cTnC orthologs (Figure 1-9). Of these 13 differences, four are considered conservative substitutions: aspartate 14, isoleucine 28, threonine 92, and valine 119 in ScTnC for glutamate 14, valine 28, serine 92, and isoleucine 119 in McTnC, respectively. The remaining nine non-conservative differences should, in theory, have a greater potential impact of altering the tertiary protein structure and function of these cTnC isoforms.

Figure 1-9. **Sequence alignments of different cTnC isoforms. ScTnC, salmonid cardiac TnC (2), McTnC, mammalian/bovine cardiac TnC (Swiss-Prot accession number P63315), and HcTnC, human cardiac TnC (Swiss-Prot accession number P63316). The differences are shown in bold print. ScTnC and McTnC are ~92% identical. The Ca^{2+} coordinating positions in each EF-hand site are shown above and the low high affinity Ca^{2+} domains are show in blue and red respectively. The helices are denoted by ~ and coordinating residues by X, Y, Z, -Y, -X, -Z.**

The cTnC sequence was previously thought to be identical among humans and other mammals such as pigs, chickens, and cows. Recently, it was shown that the human cTnC sequence differs from other mammals at residue 115; however, the effect of this substitution is unknown. In light of these sequence differences, the term McTnC used in studies prior to February 2005 to describe all mammalian cTnC isoforms is now classified as bovine cTnC (BcTnC). For consistency with previous studies, the term McTnC will be used in this proposal.

```
                                      ------Site I------
                                         X  Y  Z-Y-X  -Z
HcTnC:  1 MDDIYKAAVEQLTEEQKNEFKAAFDIFVLGAEDGCISTKELGKVMRMLGQ  50
McTnC:  1 ------------------------------------------------  50
ScTnC:  1 -N-----------D-------------IQD-------------------  50
                       ~~Helix A~~          ~~Helix B~~

                      -----Site  II------
                         X  Y  Z-Y-X  -Z
HcTnC:  51   NPTPEELQEMIDEVDEDGSGTVDFDEFLVMMVRCMKDDSK  90
McTnC:  51   ---------------------------------------  90
ScTnC:  51   ---------------------------------------  90
             ~~Helix C~~          ~~Helix  D~~

                     ------Site III------
                        X  Y  Z-Y-X  -Z
HcTnC:   91  GKSEEELSDLFRMFDKNADGYIDLDELKIMLQATGET  127
McTnC:   91  ----------------------E----------------  127
ScTnC:   91  --T----A---C-----------Q---V--E----A  127
             ~~Helix  E~~          ~~Helix F~~

                      ------Site  IV------
                         X  Y  Z-Y-X  -Z
HcTnC:  128   ITEDDIEELMKDGDKNNDGRIDYDEFLEFMKGVE 161
McTnC:  128   --------------------------------- 161
ScTnC:  128   -------------------K------------- 161
              ~~Helix G~~          ~~Helix  H~~
```

It is interesting to note that there is no naturally occurring tryptophan in cTnC. There is complete sequence identity in the site II low affinity-binding region (residues 52-84) of McTnC and ScTnC. This suggests that sequence differences in locations other than site II may be functionally significant and these variations are found to exist in two main regions. The first region is in the N-terminal non-functional site I (residues 1-29), contains five sequence differences. The three non-conservative substitutions in this area are asparagine 2 in ScTnC instead of aspartic acid, glutamine 29 instead of leucine, and aspartic acid 30 instead of glycine. The presence of the negatively charged asparagine in residue 2 may affect the tertiary structure of the N-terminus α-helical overhang (residue 1-10) and changes to the protein sequence in this location could affect the protein binding function in site II (*45*). The presence of a hydrophilic side group in glutamine and negatively charged aspartic acid in the helix-loop-helix of ScTnC may impact the structural function of the protein. The 3D NMR solution structures of truncated N-terminus McTnC and ScTnC at 30 °C also show a subtle difference in protein folding, indicating structural variations due to sequence differences (*46*). Although site I is nonfunctional in cTnC, manipulations in this region have been shown to have a significant allosteric effect on Ca^{2+} affinity both *in vitro* (*2, 47, 48*) and *in situ* (*47, 49*). This domain is also suggested to be actively engaged in protein contraction; site I moves when site II is titrated with Ca^{2+} (*45, 50*). The truncated N-terminus McTnC and ScTnC demonstrated the same difference in Ca^{2+} affinity compared to the full-length proteins *in vitro* postulating this domain to be the main determinant of Ca^{2+} binding (*2*).

The second area of sequence variation occurs in the site III high affinity Ca^{2+} or Mg^{2+} binding region (residues 92-124), which contains seven amino acid substitutions.

Site III of TnC binds to the inhibitory domain of TnI upon activation (*51, 52*) and has been shown to be dependent on charge and hydrophobic interactions (*53*). The difference of these orthologs in the C terminus may effect cTnC interaction with cTnI during contraction and subsequently how cTnC binds Ca^{2+} *in situ*.

1.9 Fluorescence reporters

Fluorescence spectroscopy is a common analytical method used to study active proteins in solution, in crystal state, and in membranes. It also provides the added benefit of high sensitivity, allowing one to work at micromolar (10^{-6} M) concentrations typical of *in situ* conditions. The assays take advantage of the fluorescent properties of aromatic ring structures such as, phenylalanine, tyrosine, and tryptophan. However, the use of such probes becomes limited when more than one residue with an aromatic ring is present. With the use of site-directed mutagenesis techniques, these fluorescence probes can be incorporated into a designated site of a protein to provide considerable insight on protein conformational changes. It is imperative to insert the reporter into a position that does not compromise the functional ability of the molecule yet still is able to report conformational changes. However, the incorporation of a tryptophan probe will result in a relatively low signal-to-noise ratio due to the presence of numerous other proteins containing tryptophans in an *in situ* environment. In this case, introduction of non-natural fluorescence probes into the molecule is a viable alternative.

It has been shown that natural tryptophan analogues such as 5-hydroxytryptophan (5HW) and artificial ones such as 7-azatryptophan (7ZW) have unique spectral properties (Table 1-1). These analogues can be incorporated into proteins in place of tryptophan to

produce a unique fluorescence profile (*35, 54, 55*). The emission and excitation spectra of 5HW and 7ZW are right shifted to that of tryptophan which allows for readily distinguishing these signals in the presence of multiple tryptophans. Each of these two reporters has its own advantages. 7ZW is preferred over 5HW due to its longer emission wavelength, which reduces the possibility of detecting a tryptophan emission where as 5HW is preferred over 7ZW due to its higher quantum yield.

Schlesinger (*56*) was the first to purify alkaline phosphates in which the tryptophan were replaced by 2-azatryptophan or 7-azatryptophan using a tryptophan auxotrophic *E.coli*. Schlesinger (*56*) also observed that the tryptophan analogues had little effect on the structure and function of the enzyme, but had a significant effect in the absorbance and fluorescence properties. Barlati and Ciferri (*57*) later successfully incorporated tryptophan analogues into proteins. However, it was not until 1986 that Ludescher et al (*58*) first demonstrated the possible use of tryptophan analogues as probes in fluorescence spectroscopy.

Current molecular biology techniques make it possible to achieve a high incorporation rate of tryptophan *in situ* through the use of an auxotroph, an organism that requires a specific growth substance for normal metabolism and reproduction. The use of an auxotroph will force the cells to use the residue provided in the medium for growth.

Table 1-1. Excitation, peak emission, and quantum yield of tryptophan, 7-azatryptophan (7ZW), and 5-hydroxytryptophan (5HW).

	Tryptophan	7-azatryptophan (7ZW)	5-hydroxytryptophan (5HW)
Excitation λ (nm)	276	315	315
Peak Emission λ (nm)	330	380	340
***Quantum Yield, Φ**	0.130	0.016	0.256
Molecular Weight (Daltons)	204.2	205.2	220.2

* Quantum yields are with excitation at 280 nm.
Data sources: (*59*), (*2*), and (*54*).

Figure 1-10. Chemical structures of L-Tryptophan and L-7-Azatryptophan.

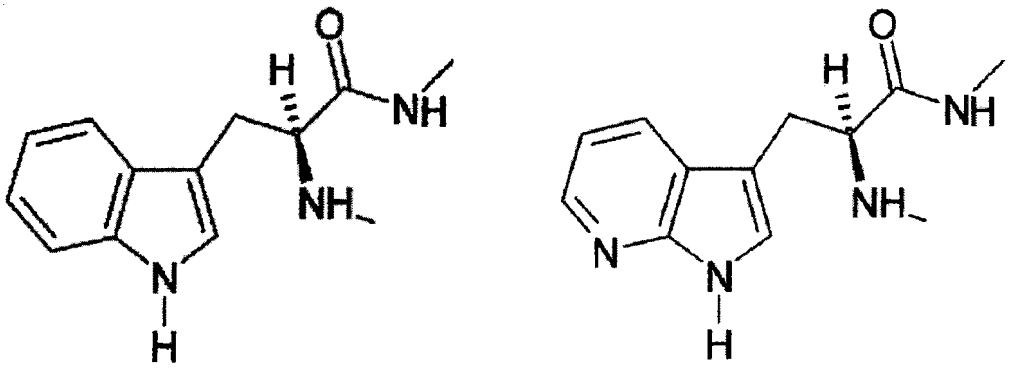

L-Tryptophan **L-7-Azatryptophan**

2. OBJECTIVES AND HYPOTHESES

The overall objective of this study is to identify the specific residues responsible for the higher Ca^{2+} affinity in ScTnC *in vitro* and to then determine if the same effect is observed in single skinned mammalian cardiac myocytes. The understanding of the mechanism of the increased sensitivity of ScTnC could provide valuable information in the development of new therapeutic targets for treating heart failure. The specific objectives and hypotheses are as follows:

1) Identify residues responsible for higher Ca^{2+} binding affinity in full length ScTnC.
   - L29Q McTnC which is related to Familial Hypertrophic Cardiomyopathy (FHC) will increase the Ca^{2+} binding affinity of TnC
   - D2N/V28I/L29Q/G30D (NIQD) residues in ScTnC are responsible for its higher Ca^{2+} binding affinity and sensitivity

2) Reconfirm the regulatory role of N-terminus TnC through the creation of an N-terminus skeletal- C-terminus cardiac TnC chimera.
   - Chimeric TnC will possess similar Ca^{2+} binding affinity as skeletal RsTnC
   - Chimeric TnC will possess significantly different Ca^{2+} sensitivity as McTnC

3) Relate changes in Ca^{2+} binding affinity with changes in Ca^{2+} k_{on} and k_{off} *in vitro*.
   - Higher Ca^{2+} binding affinity results from an increased k_{on} and/or decreased k_{off}

4) Relate changes in Ca^{2+} binding affinity with changes in Ca^{2+} sensitivity *in situ*.
   - Changes in Ca^{2+} binding affinity of TnC will alter the Ca^{2+} sensitivity of the cell in a parallel manner

5) Explore the efficient of use of the non-natural 7-azatryptophan (7ZW) as a fluorescence reporter to measure Ca^{2+} binding to TnC.
    - 7ZW will effectively report Ca^{2+} binding to TnC both *in vitro* and *in situ*.

3. EXPERIMENTAL DESIGN

3.1 *In vitro* Ca^{2+} binding affinity and properties

In the *in vitro* approach, steady state spectrofluorometry was performed in conjunction with stopped-flow analysis to obtain data on the K_d, k_{on}, and k_{off} of Ca^{2+} binding to various TnC mutants with altered Ca^{2+} affinity. These parameters are evaluated in TnC by replacing the native phenylalanine at position 27 with either a tryptophan or an engineered 7-azatryptophan that serve as unique fluorescent reporters. Although this residue resides near site I, it reports on the site II Ca^{2+} binding site (*50, 54, 60*). In this study, tryptophan is chosen as the reporter for a number of reasons. First and most importantly, tryptophan is not naturally found in TnC and the creation of a tryptophan at residue 27 of McTnC and ScTnC has been proven to be an effective reporter for Ca^{2+} binding without significantly affecting its general structure (*60*). The second advantage of using tryptophan is its higher quantum yield compared to phenylalanine and tyrosine. 7ZW is chosen over 5HW due to its greater Stokes shift (longer emission wavelength), which reduces the possibility of detecting a tryptophan emission in future *in situ* experiment. Although residue 27 occurs in site I, it reports on the site II Ca^{2+} binding site (*50, 54, 60*). The binding of Ca^{2+} to site II increases the relative fluorescence of the probe resulting in detectable change in emission intensity.

Fluorescence spectrofluorometery was performed as a function of pCa under steady-state conditions to determine the Ca^{2+} binding characteristic of different isoforms of TnC, mutant TnC, and chimeric TnC. Tryptophan and 7ZW containing TnC

molecules were excited at 276nm and 315 nm, respectively and the fluorescence emissions were monitored at 330 nm and 380 nm, respectively. The Ca^{2+} affinities of the proteins were reported as $K_{fl/2}$ (pCa at half-maximal fluorescence). *In situ* single fibre replacements were then carried out on designer TnC that altered Ca^{2+} affinity.

Stopped-flow measurements and protein exposure to Artificial Ca^{2+} Transients (ACTs) were performed by Dr. Jonathan Davis' group at the Ohio State University as a function of time against changes in tryptophan fluorescent or changes in percentage transient occupancy of Ca^{2+}, respectively to determine the k_{off}, k_{on}, and K_d of Ca^{2+} binding to McTnC, ScTnC, and mutant McTnC. Tryptophan containing TnC molecules were excited at 276 nm and the fluorescence emissions were monitored at 330 nm.

3.2 *In situ* reconstitution of cardiac TnC using single cardiomyocytes

The *in situ* approach refers to the TnC being in its functional position on the thin filament where it interacts with numerous proteins including TnI and TnT. This component is critical because K_d of the Ca^{2+} binding sites on TnC is allosterically affected by its interaction with other proteins on the thin filament. In addition, the length dependence of TnC Ca^{2+} binding cannot be studied *in vitro*. The various TnC mutants were reconstituted into single skinned cardiomyocytes and we were able to monitor tension generation and sarcomere length while the cell was contracting isometrically.

One of the biggest advantages of TnC reconstitution into single skinned cardiac myocytes is that it can allow for more rigorous control over sarcomere length and Ca^{2+} concentration, thus eliminating the complicating effect of changes in sarcomere length on

force generation. Effective control of sarcomere length cannot be adequately achieved in a multicellular preparation because the sarcomere length will have to be averaged throughout the preparation with a large degree of sarcomere length heterogeneity. Another major advantage is the ability to examine an important component of Frank-Starling relationship, the length dependency of Ca^{2+} binding in TnC which is unfeasible *in vitro*. By using single cells, we were able to minimize the effect of sarcomere length on Ca^{2+} sensitivity and test the effects of the TnC mutants within the troponin complex. The Ca^{2+} sensitivities of the proteins were reported in terms of $K_{F1/2}$ (pCa at half-maximal force). We also tested the effect of 7ZW at residue 27 of TnC. This unnatural amino acid has special fluorescent properties that can be used in future experiments to monitor Ca^{2+} binding to TnC and the force generation simultaneously, which has not been achieved before.

4. METHODS

4.1 TnC expression vector

The McTnC and ScTnC cDNA subcloned into the pGex (Stratagene, La Jolla, CA) vectors were supplied by Gillis et al (*1*). Proteins used in the early part of this study were purified using the pGex system. We later switched to using the pET system (Novagen, San Diego, CA) which has been found to provide a higher protein yield. The cDNA from Gillis et al (*1*) were subcloned into pET 21a+ vectors (Novagen, San Diego, CA) and the RsTnC cDNA in the pET 24a+ expression vector had been supplied by Dr. Michael Regnier's group from University of Washington. The two pET vectors differ only in antibiotic resistance; pET 21a+ is ampicillin resistant while pET 24a+ is kanamycin resistant.

4.2 Subcloning into the pET system

The McTnC and ScTnC cDNA in the pGex plasmid (*1*) were subcloned into the pET 21a+ expression vector. Restriction enzymes NdeI and EcoRI (New England Biolabs, Pickering, ON) were used to digest the pGex vector for McTnC and ScTnC extraction. The pET 21a+ vector was digested in a similar manner. Following digestion, the cassette and plasmids were purified by gel electrophoresis using a 1% agarose gel. The band corresponding to the correct size of the nucleotide sequence was extracted from the gel and purified using a Gel Extraction kit (Qiagen, Mississauga, ON). The cassette

and the plasmids were ligated using T4 DNA ligase (Gibco BRL, Gaithersburg, MD). The correct insertion of the clones into the vector was confirmed through sequencing by the CMMT/BCRI DNA Sequencing Core Facility (Vancouver, B.C).

4.3 Construction of TnC mutants

Mutations were performed the same way on TnC in the pGex and pET vector. The parental cDNA inserts of McTnC and ScTnC were used as template for the extension of sense and antisense oligonucleotide primers containing codons to create the desired mutations using the QuikChange site-directed mutagenesis kit (Stratagene, La Jolla, CA).

The nucleotide sequences were confirmed by sequencing. Once the sequence of IQD McTnC was ascertained, it was used as the template for the extension of D2N oligonucleotide primers containing codons to create the NIQD McTnC mutant. The VLD ScTnC was used as the template for the extension of N2D oligonucleotide primers containing codons to create the DVLG ScTnC mutant. The sequences of the mutations were all confirmed at the CMMT/BCRI DNA Sequencing Core Facility.

Figure 4-1. Sequence of the oligonucleotide primers use in creating RsTnC mutant.

F27W RsTnC sense:
GCCGCCTTCGACATGTGGGATGCTGATGGCGGTGG;
F27W RsTnC antisense:
CCACCGCCATCAGCATCCCACATGTCGAAGGCGGC;

Figure 4-2. Sequences of the oligonucleotide primers used in creating McTnC mutants.

F27W McTnC sense:
GCCTTCGACATCTGGGTGCTGGGGGCAGAGGATGGCTGC;
F27W McTnC antisense:
GCAGCCATCCTCTGCCCCCAGCACCCAGATGTCGAAGGC;

D2N McTnC sense:
GGAGATATACATATGAATGACATCTATAAGGCGGCG;
D2N McTnC antisense:
CGCCGCCTTATAGATGTCATTCATATGTATATCTCC;

L29Q McTnC sense:
GCCTTCGACATCTTCGTGCAGGGGGCAGAGGATGGC;
L29Q McTnC antisense:
GCCATCCTCTGCCCCCTGCACGAAGATGTCGAAGGC;

F27W L29Q McTnC sense:
GCCTTCGACATCTGGGTGCAGGGGGCAGAGGATGGCTGC;
F27W L29Q McTnC antisense:
GCAGCCATCCTCTGCCCCCTGCACCCAGATGTCGAAGGC;

V28I/L29Q/G30D (IQD) McTnC sense:
GCTGCCTTCGACATCTTTATCCAGGATGCAGAGGATGGCTGC;
V28I/L29Q/G30D (IQD) McTnC antisense:
GCAGCCATCCTCTGCATCCTGGATAAAGATGTCGAAGGCAGC;

F27W V28I/L29Q/G30D (IQD) McTnC sense:
GCTGCCTTCGACATCTGGATCCAGGATGCAGAGGATGGCTGC;
F27W V28I/L29Q/G30D (IQD) McTnC antisense:
GCAGCCATCCTCTGCATCCTGGATCCAGATGTCGAAGGCAGC.

Figure 4-3. Sequence of the oligonucleotide primers used in creating ScTnC mutants.

```
F27W ScTnC sense:
GCGGCCTTTGACATCTGGATCCAGGATGCGGAGGAC;
F27W ScTnC antisense:
GTCCTCCGCATCCTGGATCCAGATGTCAAAGGCCGC;

N2D ScTnC sense:
GGAGATATACATATGGACGACATCTACAAAGCCGCG;
N2D ScTnC antisense:
CGCGGCTTTGTAGATGTCGTCCATATGTATATCTCC;

I28V/Q29L/D30G (VLG) ScTnC sense:
GCCTTTGACATCTTCGTCCTGGGTGCGGAGGACGGC;
I28V/Q29L/D30G (VLG) ScTnC antisense:
GCCGTCCTCCGCACCCAGGACGAAGATGTCAAAGGC;

F27W I28V/Q29L/D30G (VLG) ScTnC sense:
GCCTTTGACATCTGGGTCCTGGGTGCGGAGGACGGC;
F27W I28V/Q29L/D30G (VLG) ScTnC antisense:
GCCGTCCTCCGCACCCAGGACCCAGATGTCAAAGGC.
```

4.4 Construction of the skeletal-cardiac TnC chimera

An EcoRI restriction site was created as a silent mutation in McTnC at residue 76. Restriction enzymes NdeI and XhoI (New England Biolabs, Pickering, ON) were used to digest the above mutated vector for McTnC extraction. The pET 21a+ vector containing McTnC was digested in a similar manner. Following digestion, the cassette and plasmids were purified by gel electrophoresis using a 1% agarose gel. The band corresponding to the correct size of the nucleotide sequence was extracted from the gel and purified using a Gel Extraction kit. The cassette and the plasmids were ligated using T4 DNA ligase and the sequence of the insert was confirmed at the CMMT/BCRI DNA Sequencing Core Facility. An EcoRI restriction site was also introduced as a silent mutation in RsTnC at residues 75. These mutations created two EcoRI sites encoding the C-terminus of

McTnC and RsTnC. Restriction enzyme EcoRI was used to digest the above mutated vectors. The pET 24a+ vector containing N-terminus RsTnC served as the plasmid and was ligated with the C-terminus McTnC. Finally, C83Q and D86E mutations were made to create a skeletal (residues 1-87) and cardiac (88-160) TnC chimera. Sequences of all the mutations were confirmed at the CMMT/BCRI DNA Sequencing Core Facility.

Figure 4-4. Sequence of the proposed skeletal-cardiac TnC chimera.

```
Chimeric TnC:   1   MTDQQAEARSYLSEEMIAEFKAAFDMFDAI   30
Chimeric TnC:  31   GGGDISVKELGTVMRMLGQTPTKEELDAI   59
Chimeric TnC:  60   IEEVDEDGSGTIDFEEFLVMMVRQMKED   87
Chimeric TnC:  88   SKGKSEEELSDLFRMFDKNADGYIDLEELKIMLQAT  123
Chimeric TnC: 124   GETITEDDIEELMKDGDKNNDGRIDYDEFLEFMKGVE  160
```

Figure 4-5. Sequence of the ologinucleotide primers use in creating skeletal-cardiac TnC chimera.

```
E76E McTnC sense:
GGCACTGTGGACTTTGATGAATTCCTTGTTATGATGGTTCGG;
E76E McTnC antisense:
CCGAACCATCATAACAAGGAATTCATCAAAGTCCACAGTGCC;

E75E RsTnC sense:
GGCACCATCGACTTCGAGGAATTCTTGGTCATGATGGTGCGC;
E75E RsTnC antisense:
GCGCACCATCATGACCAAGAATTCCTCGAAGTCGATGGTGCC;

C83Q + D86E chimeric TnC sense:
GTTATGATGGTTCGGCAGATGAAAGAGGACAGCAAAGG;
C83Q + D86E chimeric TnC antisense
CCTTTGCTGTCCTCTTTCATCTGCCGAACCATCATAAC.
```

4.5 Protein expression and purification using the pGex system

The pGex vectors containing the McTnC F27W and ScTnC F27W in *Escherichia coli* strain BL21 (DE3) cells (Novagen, San Diego, CA) were provided by Gillis et al (*1*). The pGex expression vectors containing various McTnC F27W mutation inserts were transformed into *Escherichia coli* strain BL21 (DE3) cells. In brief, the GST-fusion protein was purified according to the manufacture's recommendation as follows. 50 ml of bacto-trypthone and yeast extract (TY) media plus ampicillin (100 µl final concentrations) was inoculated with the bacteria overnight at 37 °C to serve as inoculum for 2X 1L of TY media plus ampicillin. The culture was allowed to grow for approximately 4 hours to cell density that gave a ~ 0.6 absorbance at 600 nm (A_{600}). To induce protein expression, isopropyl-1-thio-β-D-galactoside (IPTG) (Invitrogen, Burlington, ON) was added to a final concentration of 0.1 mM. After 4 hours, centrifugation (6,000 rpm for 15 min) at 4°C was performed to precipitate the cells from the culture supernatant. Cells pellets were resuspended in ice-cold phosphate buffered saline (PBS, 140 mM NaCl, 2.7 mM KCl, 10 mM Na_2HPO_4, 1.8 mM KH_2PO_4, pH 7.3) and stored frozen at - 80 °C until needed. The cell pellets were thawed and sonicated using a Vibra-Cell sonicator (Sonics and Materials, Canbury, CT), followed by 1% final concentration of Triton X-100 treatment to further solubilize the proteins. The cell lysates were then centrifuged (12,000 rpm for 15 min) to remove cellular debris. The cell supernatants from the 2L culture were pooled, sterilize filtered, and applied directly to a 1.5 x 2 cm glutathione-Sepharose 4B column (Pharmacia Biotech, Piscataway, NJ) equilibrated with PBS. After loading, the column was washed with 30 bed volumes of PBS and then equilibrated with *buffer 1* (50 mM Tris-HCl, 100 mM NaCl, 5 mM $CaCl_2$,

pH 8.0). To separate the GST fusion protein, 0.1 mg of serine protease factor Xa (Novagen, San Diego, CA) in 4 ml *buffer 1* was applied and allowed to remain on the column overnight at room temperature. The next day, free recombinant cTnC was collected by passing 10 × bed volumes of *buffer 1*. One EDTA-free Protease inhibitor cocktail mini-tablet (Roche, Mississauga, ON) was added to every 35 ml of pooled column fractions. The pooled column fractions were then dialyzed overnight against 2L *buffer 2* (50 mM Tris, 15 mM $CaCl_2$, 1 mM DTT, 500 mM NaCl, pH 7.5) with three changes. The dialyzed fraction was applied directly to a 2.6 × 4.5 cm column packed with phenyl Sepharose 6 Fast Flow, high sub (Pharmacia Biotech, Piscataway, NJ) equilibrated with *buffer 2*. After loading, the column was washed with 100 ml of *buffer 2* and then with 100 ml of *buffer 2* without NaCl; this cycle was repeated a total of 3 times. Recombinant cTnC was then eluted with *buffer 3* (50 mM Tris, 15 mM EDTA, 1 mM DTT, pH 7.5), dialyzed overnight against 100 × of HPLC-grade water with three changes, lyophilized, and stored frozen at – 80 ° C until needed. The purity and atomic masses of lyophilized proteins were confirmed by Matrix Assisted Laser Desorption/Ionization-Time-of-flight Mass Spectrometry (MALDI-TOF MS) at the UBC Mass Spectrometry Centre (Vancouver, BC).

4.6 Protein expression and purification using the pET system

The pET 21a+ vector containing McTnC and ScTnC constructs and pET 24a+ vector containing RsTnC and chimeric TnC constructs were transformed into *Escherichia coli* strain BL21 (DE3) cells. The pET 21a+ is ampicillin resistant while pET 24a+ is kanamycin resistant. In brief, the protein expression and purification were as follows. A 50 ml of Luria-Bertani (LB) media plus antibiotic (100μM ampicillin or 50 μM kanamycin final concentrations) were inoculated with bacteria and allowed to grow overnight at 37 °C. The culture served as an inoculum for 4 × 1L of LB plus antibiotic. Once inoculated, the culture was allowed to grow to a cell density that gave a ~ 0.6 absorbance at 600 nm (A_{600}). To induce protein expression, isopropyl-1-thio-β-D-galactoside (IPTG) was added to a final concentration of 1 mM. After 4 hours, centrifugation (7,000 rpm for 15 min) was performed at 4 °C to precipitate the cells from the culture supernatant. Cell pellets were resuspended in *buffer A* (50 mM Tris, 2 mM EDTA, 1mM DTT, 1 mM PMSF, EDTA-free complete mini tablets, pH 7.5) and stored at –80° C until needed. The cell pellets were thawed and sonicated using a Vibra-Cell sonicator. The cell lysates were then centrifuged (12,000 rpm for 15 min) to remove cellular debris. Ammonium sulphate (2.65 M final concentration) was added to the supernatant and allowed to stir at 4 °C for 30 min to allow for ammonium precipitation. The suspension was centrifuged (12,000 rpm for 30 min) to remove cellular debris. The supernatants isolated were pooled and dialyzed overnight against 2 L of *buffer B* (6 M urea, 25 mM Tris, 1mM EDTA, 15 mM β-Mercaptoethanol, pH 8.0) with three changes. The dialyzed supernatant was then applied directly to a 2.6 × 20 cm column packed with diethylaminoethyl cellulose 52-anion exchanger (Whatman, Florham Park, NJ)

equilibrated in 3 column volumes of *buffer B*. The outflow from the column was monitored by ÄKTA FPLC UPC 900 (Amersham Biosciences, Piscataway, NJ). After protein loading, the column was washed with one column volume of *buffer B* before a salt gradient (*buffer B* with 350 mM KCl) is applied. TnC was usually eluted at ~ 80% high salt concentration. Column fractions were run on a SDS-PAGE to identify desired proteins and fractions containing TnC were pooled and dialyzed overnight against 100 × of HPLC-grade water with three changes, lyophilized, and stored frozen at –80 ° C until needed. The purity and atomic masses of lyophilized proteins were confirmed by MALDI-TOF MS at the UBC Mass Spectrometry Centre.

4.7 Protein expression and purification of 7ZW TnC

The protein expression for F27ZW TnC was carried out as follows. The pET 21a+ vector containing McTnC constructs and pET 24a+ vector containing the chimeric TnC construct were transformed into CY(DE3)pLysS cells provided by Dr. Chuck Farah's group from Universidade de São Paulo, Brazil. A 50 ml of LB media plus antibiotic (100 μM ampicillin or 50 μM kanamycin final concentrations) were inoculated with bacteria in the morning at 37 °C. At the end of the day, the culture served as an inoculum for 4 × 1000 ml of *medium A* (M9 minimal medium, 20 μg/ml chloramphenicol, 5 mg/L thiamine, 20 μg/ml L-tryptophan, and 200 μg/ml appropriate antibiotic). Once inoculated, the culture was allowed to grow overnight to a cell density that gave a ~ 1.0 absorbance at 600 nm (A_{600}). Centrifugation (5,000 rpm for 10 min) was then performed at 4 °C to precipitate the cells from the culture supernatant. Cells

pellets were resuspended in 4 × 1000 ml *medium B* (M9 minimal medium, 20 μg/ml chloramphenicol, 5 mg/L thiamine, 1.0 mM IPTG, 200 μg/ml 7-DL-azatryptophan, and 200 μg/ml appropriate antibiotics) and allowed to grow for 4 hours with vigorous shaking. Centrifugation (7,000 rpm for 15 min) was performed at 4 °C to precipitate the cells from the culture supernatant. Cell pellets were resuspended in *buffer A.* The subsequent purification procedures were identical to section 4.6.

4.8 Estimation of 7ZW incorporation in TnC F27ZW

Due to the 1 dalton difference in the molecular weights of tryptophan and 7ZW, the only way to estimate 7ZW incorporation is by a comparative analysis of absorbance and emission spectra of the TnC F27W and F27ZW proteins. The estimation method used was as described by Valencia et al (*54*). The emission spectra scan was obtained on TnC F27W, TnC F27ZW, and TnC proteins at 287 nm and 315 nm excitation. The emission spectra were normalized by subtracting the TnC emission spectrum to discount the contribution of phenylalanines. The two normalized F27ZW emission spectra obtained at 287 nm and 315 nm excitation were subtracted, and the difference (a small peak at ~ 340 nm) was transformed back to absolute values. This area was compared to a sample of known F27W concentration and assumed to represent the amount of F27W contaminating the F27ZW sample.

4.9 Steady state Ca^{2+} titration

Steady state fluorescence spectroscopy was performed using a SLM Instruments (Urbana, IL) 4800 Aminco fluorometer equipped with a thermostated cell assemble attached to a NesLab (Portsmouth, NJ) water bath to maintain the cuvette at 21.0 ± 0.1 °C. The solution used was 1.0 mM EGTA, 30 nM $CaCl_2$, 112.0 mM KCl, and 50 mM MOPS (*2*). Ca^{2+} concentrations ranging from pCa values of 4.5 to 8 were used to titrate various TnC molecules. The data were analyzed as described in Gillis et al (*1*). The fluorescence measurements from each titration were fitted using the Hill equation : $f = f_{max} [Ca^{2+}]^{nH}/(k^{nH} + (Ca^{2+})^{nH})$, where f is the relative fluorescence, f_{max} is the maximum Ca^{2+} dependent fluorescence equal to 1, n_H is the Hill coefficient and k corresponds to the $[Ca^{2+}]$ at half-maximal Ca^{2+} dependent fluorescence ($K_{f½}$) using Origin 6.0 (Microcal Software, Northhampton, MA). The data were analyzed statistically using a one-way repeated measures Analysis of Variance between groups (ANOVA) followed by Bonferroni *post hoc* test. The values of $K_{f½}$ are reported as means ± SE in pCa units. Two means were considered to be not significantly different when the P value was greater than 0.05.

4.10 Ca^{2+} binding properties of TnC and mutants

These data were collected in collaboration with Dr. Jonathan Davis' group at the Ohio State University in which we provided the proteins and they performed the fluorescent measurements. The methods used were as described in Davis et al (*15, 61*). The Ca^{2+} k_{off} data from the regulatory domain of the cTnC F27W proteins were measured using an applied Photophysics Ltd. (Leather-head, UK) model SX. 18 MV stopped-flow instrument with a dead time of 1.6 ms at 15 °C and 5 °C. Each cTnC F27W proteins

(2 μM) was mixed with 500 μM of Ca^{2+} in 10 mM MOPS, 90 mM KCl, 1 mM DTT, pH 7.0 in the presence of 3 μM $MgCl_2$ was rapidly mixed with an equal volume of 10 mM EGTA in the same buffer. The cTnC F27W samples were excited at 276 nm using a 150-W xenon arc source and the emission was monitored at 330 nm through a UV-transmitting black glass filter (UG1) from Oriel (Stratford, CT). The data were fitted using a program that utilizes the nonlinear Levenberg-Marquardt algorithm by P.J. King (Applied Photophysics Ltd.). Each Ca^{2+} k_{off} value represents an average of at least three separate experiments with each averaging at least five traces fit with a single exponential equation (variance $< 8 \times 10^{-4}$). These k_{off} data were used to calculate the temperature coefficient Q_{10} for the cTnC F27W proteins using the equation $Q_{10} = (k_{off}$ at 15 °C) / (k_{off} at 5 °C).

The cTnC F27W proteins were exposed to ACTs to estimate the Ca^{2+} k_{on} to cTnC. Various amplitudes and durations of ACTs were generated in a stopped-flow apparatus by rapidly mixing one solution of known concentration of Ca^{2+} with another solution of known concentration of Ca^{2+} chelator (EGTA was used in this experiment) (*15, 62*). The buffer used was 10 mM MOPS, 90 mM KCl, 1 mM DTT, 3 mM $MgCl_2$, pH 7.0 (*15*). ACT was generated by rapidly mixing each cTnC F27W protein (2 μM) with 1 mM EGTA in buffer against buffer with increasing Ca^{2+} concentrations from 10 μM to 5000 μM. Before mixing, the N-terminus of cTnC was in its apo state. After mixing and prior to EGTA removing Ca^{2+} from the protein and chelating free Ca^{2+}, the N-terminus of the cTnC F27W proteins were transiently occupied by Ca^{2+}. For each ACT, the percentage of transiently occupancy trace of each cTnC F27W protein was determined at selected

time points typically ≥2 ms after mixing is completed. Each transient occupancy trace is an average of 3 separate experiments with each averaging at least 10 separate traces.

Computer simulations were then carried out using KSIM version 1.1 (N.C. Millar, UCLA School of Medicine, Los Angeles, CA) to estimate the Ca^{2+} k_{on} for each cTnC F27W (*15, 63*). This computer modelling solved the equation: cTnC F27W + Ca^{2+} ↔ cTnC F27W·Ca^{2+} using the Runge-Kutta method. The equation was regarded as bimolecular and reversible. Initial concentrations of the reagents in the simulations were set at the steady state value of the 2 stopped-flow syringes immediately after mixing (time = 0). The Ca^{2+} k_{off} value was set at that of simulating protein and then the Ca^{2+} k_{on} were allowed to vary until the modelled transient occupancy approximated the experimental data, taking into account the experimental error. The final simulated Ca^{2+} k_{on} for each cTnC F27W protein was calculated as a mean of k_{on} for each individual trace ± S.D.

The Ca^{2+} K_d were calculated using the equation $K_d = k_{off}/k_{on}$, where k_{off} represent the single release of Ca^{2+} ion and K_d represent the binding event of a single Ca^{2+} ion to the N-terminus of cTnC as described in (*64*).

4.11 Cardiac TnC extraction and reconstitution

Different isoforms of TnC, mutant TnC, and chimeric TnC were reconstructed into chemically skinned cardiomyocytes. Ventricular myocytes was obtained by enzymatic digestions of adult hearts from mouse *(47)*. In brief, mouse weighing 30 to 40 g were anesthetized (intravenous pentobarbital sodium 40 mg/kg) and heparinized (intravenous 1000 IU/ kg). The heart of the animal was excised and immersed in an ice-

cold nominally Ca^{2+} free solution (100 mM NaCl, 10 mM KCl, 1.2 mM KH_2PO_4, 5 mM $MgSO_4$, 50 mM taurine, 20 mM glucose, 10 mM HEPES, pH 7.2). The heart was then cannulated via the aorta and perfused in a retrograde fashion at constant perfusion speed of 3 ml/min for 4-5 minutes. After all the blood had been washed out, the heart was cannulated at 37°C for a additional 30 minutes with nominally Ca^{2+} free solution containing 0.12 – 0.16 mg/ml collagenase (Yakult, Tokyo, Japan) then an additional 10 minutes with storage solution (120 mM $C_3H_5KNO_4$, 5mM $MgCl_2$, 20 mM taurine, 1 mM EGTA, 10 mM glucose, 10 mM HEPES, pH 7.4) containing 0.1 mg/ml type XIV protease (Sigma, Oakville, ON). The ventricle was diced up in storage solution containing 1% BSA and the cell suspension was filtered through a 100 μM nylon mesh. The pellet was washed twice using storage buffer and the cardiac myocytes were subsequently skinned by suspending the cell pellet in relaxing solution (5.70 mM $MgCl_2$, 6.31 mM Na_2ATP, 2 mM EGTA, 156 mM $C_3H_5KO_2$, 10 mM BES, 1 mM DTT, 0.1 mM leupeptin, 0.1 mM PMSF, pH 7.0) containing 0.3% Triton-X for 4 minutes. The pellet was further washed twice using cold relaxing solution. Finally, the skinned cells were re-suspended in relaxing solution and stored at 4°C.

The extracted fibre was attached in a custom made experimental chamber (Figure 4-6) (*47*) using the method by Fitzsimons et al (*65*). The myocyte was glued to the apparatus via steel pins with ≤10 μm outer diameter using Dow Corning aquarium Sealant. One end of the steel pin was attached to a Cambridge Technology (Cambridge, MA) force transducer and the other to an Aurora Scientific (Aurora, ON) 308B servo motor for control of sarcomere length. The sarcomere length of the myocyte was set to 2.1 μm. The chamber was positioned on the stage of an inverted Nikon Diaphot

microscope and the entire apparatus was mounted on an anti-vibration table. The temperature of the chamber was adjusted to 15.0 ± 0.5 °C using a Julabo (Allentown, PA) F25 water bath. Images of the myocyte were captured using a Pulnix (Sunnyvale, CA) 6710 CCD camera; Fast Fourier Transform (FFT) analyses of the digitalized striated images of the myocyte provided a means for sarcomere length measurement. Myocyte images and the output signals of the force transducer were digitized using National Instruments (Austin, TX) 1424 frame grabber and PCI-MIO-16E-1 16-bit A/D converter respectively. All the recordings were displayed and stored on a computer using custom software in LabView 6i for Windows by National Instruments. A single myocyte was gravity superperfused using a three-barrel square glass pipette 700 μm in width. A micromanipulator was attached to the pipette and stepper motor for precise pipette positioning over the myocyte. The stepper motor can rapidly switch the adjacent barrel over the myocyte within 20 ms to allow for rapid switching of solution bathing the myocyte.

Endogenous mcTnC was extracted from the cell by exposing the myocytes to 5 mM K_2EDTA, and 20 mM Tris at pH 7.2 for 5 minutes at 8 °C then another 20 minutes at 15 °C as modified from Gulati et al *(30)*. The skinned myocyte was then reconstituted by 30 minutes incubation in relaxing solution containing 10 μM of engineered TnC. Maximal Ca^{2+}-activated Force (F_{max}) at pCa 4.5 prior to extraction was used in subsequent calculations for determining the force loss and recovery due to cTnC extraction and reconstitution. Myocytes that showed altered sarcomere pattern or did not achieve 80% of the original F_{max} after the extraction/reconstitution protocol were discarded.

Ca^{2+}- activated force (F) was measured as the reconstituted myocyte was exposed to a series of solutions of increasing Ca^{2+} concentration (pCa 8.0–4.5). Each force-pCa curve was fitted with Hill equation: $F/F_{4.5} = [Ca^{2+}]^{nH}/(k^{nH} + (Ca^{2+})^{nH}]$, where n_H is the Hill coefficient and k corresponds to the $[Ca^{2+}]$ required for pCa at half-maximal force ($K_{F½}$) using Origin 6.0. The data were analyzed statistically using a one-way repeated measures analysis of variance (ANOVA) followed by Bonferroni *post hoc* test. The values of $K_{F½}$ were reported as means ± SE in pCa units. Two means were considered to be not significantly different when the P value was greater than 0.05.

Figure 4-6. **A schematic diagram of the myocyte attachment and the solution perfusion system.**
The inset photograph is a single myocyte mounted on the apparatus (1900 × magnification)

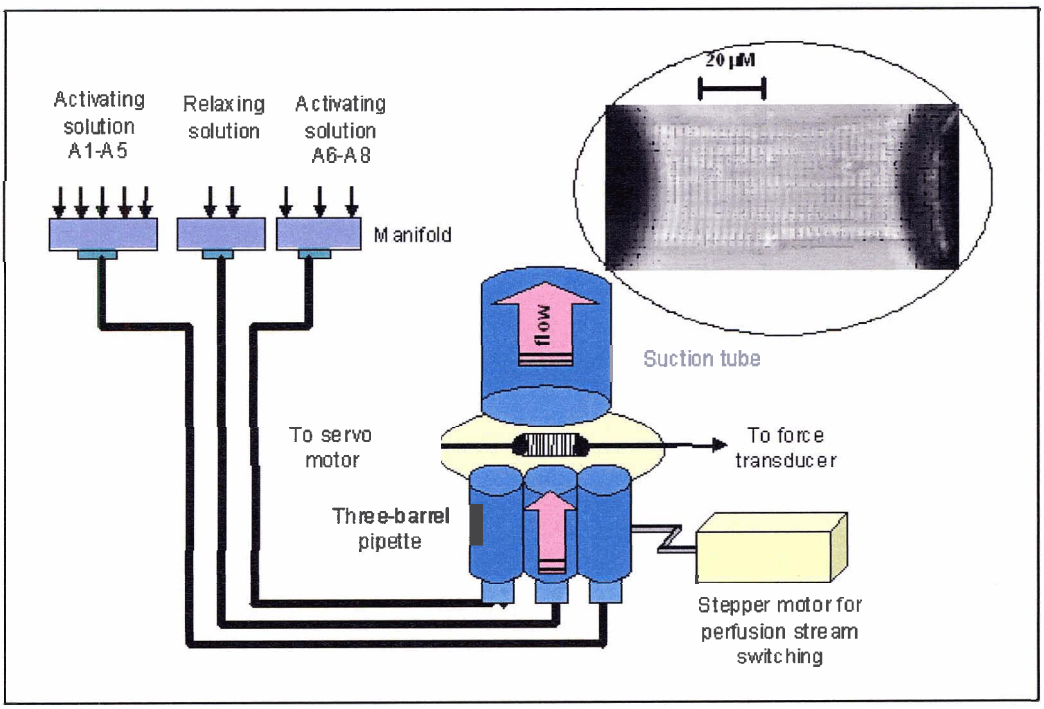

5. RESULTS

5.1 Ca^{2+} binding affinity of various TnC

There are five differences at the amino acid sequence level between the N-terminus of ScTnC (ScNTnC) and McTnC (McNTnC). These substitutions are N2, D14, I28, Q29, and D30 in ScNTnC, for D2, E2, V28, L29, and G30 in McNTnC, respectively (Figure 1-9). Results from previous studies have demonstrated that Q29 and D30 are required for the ~ 2 fold higher Ca^{2+} affinity in ScNTnC compared to McNTnC and provided indirect evidence that N2 is also required (*2*). Based on this information, the I28 substitution was chosen over the conservative D14 substitution and added to QD McNTnC F27W to create IQD McNTnC F27W. The Ca^{2+} titration curve of this mutant was left shifted indicating a slight increase in Ca^{2+} affinity compared to McNTnC F27W (Figure 5-1). The N2 substitution was subsequently added into the IQD McNTnC F27W mutant to create NIQD McNTnC F27W. Using $K_{fl/2}$ (pCa at half-maximal fluorescence) as an indicator of Ca^{2+} affinity which represents the binding event of Ca^{2+} ion to the activating site of TnC *in vitro*, the Ca^{2+} affinity of NIQD McNTnC F27W was ~ 18% higher than that of ScNTnC (*47*). These data demonstrate that N2, I28, Q29, and D30 are responsible for the high Ca^{2+} affinity of ScTnC F27W as determined *in vitro*.

Figure 5-1. **Steady state Ca^{2+} binding curves of ScNTnC F27W (n = 10), NIQD McNTnC F27W (n = 9), IQD McNTnC F27W (n = 7), and McNTnC F27W (n = 8) at 21 °C, pH 7.0.**
Data were normalized with respect to the maximal fluorescence of each Ca^{2+} titration and are presented as means ± SE. The curves were generated by fitting the data with the Hill equation.

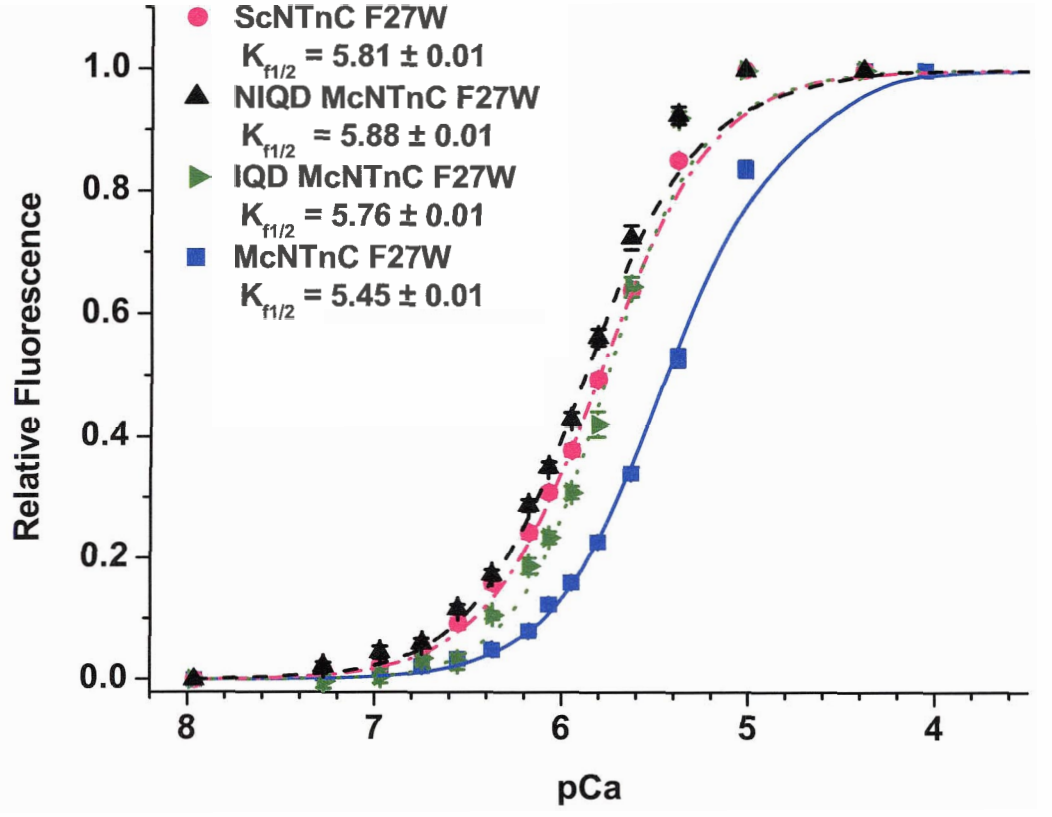

Replication of these substitutions was performed in full length McTnC and ScTnC. The Ca^{2+} affinity of the full length cTnC F27W mutants was found to be altered in a comparable manner to that of cNTnC F27W mutants. This suggests that it is only the sequence differences in the N-terminus that is involved in conferring the high Ca^{2+} affinity of site II ScTnC F27W. Previous studies also demonstrated that the removal of the C-terminus does affect the Ca^{2+} affinity of the protein, as shown in the differences in $K_{fl/2}$ values, but the affect is uniform in all mutants (*2*).

The L29Q McTnC substitution was recently suggested to be related to patients with familial hypertrophic cardiomyopathy (FHC) (*66, 67*). FHC is a primary genetic disorder characterized by increase wall thickness in the left ventricle characterized by a remarkable diversity in clinical presentations, ranging from no symptoms to severe heart failure and sudden cardiac death. This single substitution causes a slight left shift of the Ca^{2+} titration curve (Figure 5-2). Using $K_{fl/2}$ as an indicator of Ca^{2+} affinity, the Ca^{2+} affinity of L29Q McTnC F27W was ~ 32% higher than that McTnC F27W. The reciprocal substitution of this mutation, Q29L was previously performed in ScNTnC where a ~ 60% decrease in Ca^{2+} affinity was observed (*2*). These data suggest that residue 29 of cTnC plays an important role in Ca^{2+} affinity.

Figure 5-2. Steady state Ca^{2+} binding curves of ScTnC F27W (n = 8), L29Q McTnC F27W (n = 8), and McTnC F27W (n = 8) at 21 °C, pH 7.0.
Data were normalized with respect to the maximal fluorescence of each Ca^{2+} titration and are presented as means ± SE. The curves were generated by fitting the data with the Hill equation.

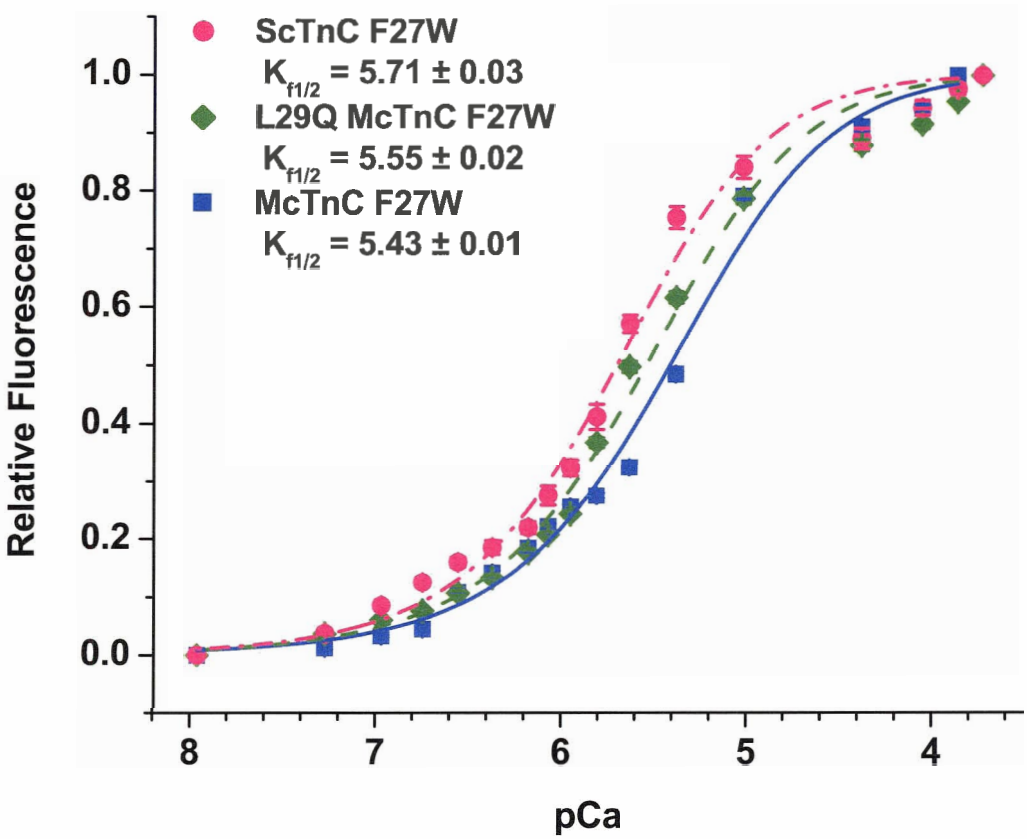

The Ca^{2+} titration curves of ScTnC F27W and NIQD McTnC F27W are virtually superimposable with a $P > 0.05$ indicating equivalent Ca^{2+} binding affinity (Figure 5–3). These data validate the hypothesis that N2, I28, Q29, and D30 are responsible for the high Ca^{2+} affinity of ScTnC F27W as determined *in vitro*.

The reciprocal substitutions of NIQD, which is DVLG were performed in ScTnC F27W to further investigate the effect of these residues on Ca^{2+} affinity of cTnC. The Ca^{2+} titration curve of the DVLG ScTnC F27W was right shifted indicating a decrease in Ca^{2+} affinity (Figure 5-4). The Ca^{2+} affinity of this mutant was only ~ 59% of McTnC F27W and ~ 31% of ScTnC F27W. These data provide further evidence that N2, I28, Q29, and D30 are responsible for the high Ca^{2+} affinity of ScTnC F27W as determined *in vitro*.

An N-terminus RsTnC and C-terminus McTnC chimera was constructed as described in the Methods section 4.4. The skeletal-cardiac chimeric TnC was designed to test the hypothesis that the regulatory Ca^{2+} binding sites on the N-terminus of TnC are the main determinant of Ca^{2+} affinity. The Ca^{2+} affinity of the chimeric TnC was found to be comparable with RsTnC with a $P > 0.05$ (Figure 5-5). This provides evidence that the N-terminus of TnC is the main determinant of Ca^{2+} affinity.

Figure 5-3. Steady state Ca^{2+} binding curves of ScTnC F27W (n = 8), NIQD McTnC F27W (n = 8), and McTnC F27W (n = 8) at 21 °C, pH 7.0.
Data were normalized with respect to the maximal fluorescence of each Ca^{2+} titration and are presented as means ± SE. The curves were generated by fitting the data with the Hill equation.

* Not significantly different from each other (P > 0.05).

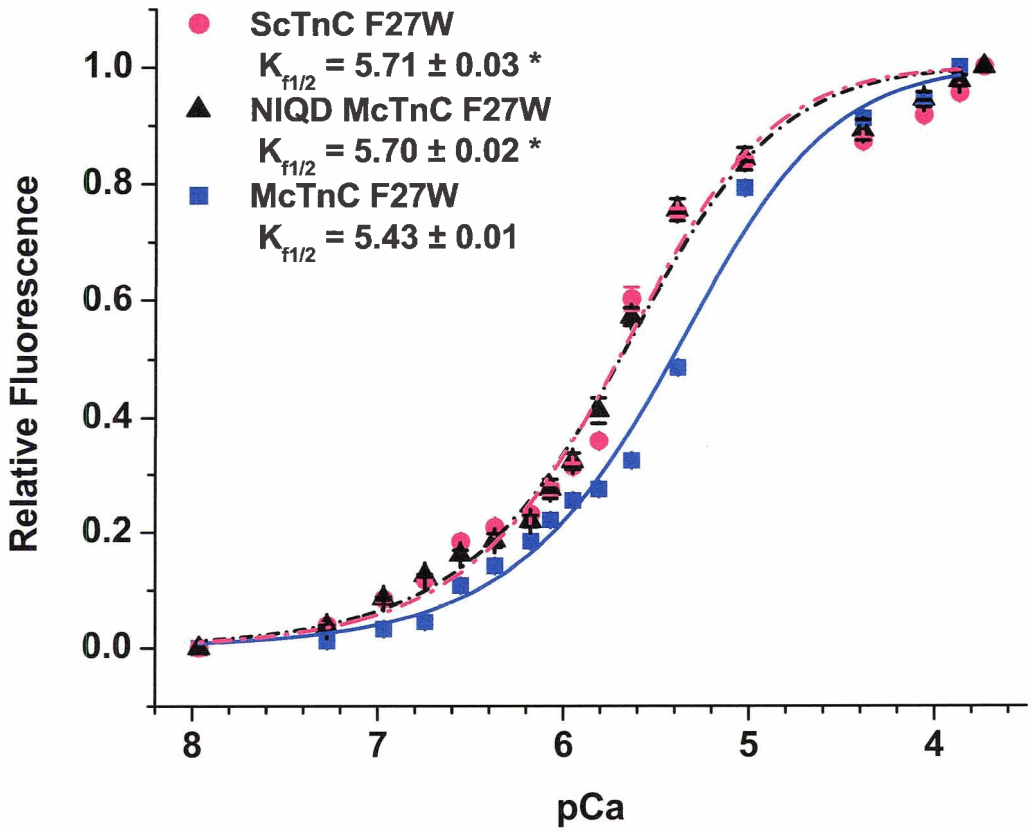

Figure 5-4. Steady state Ca^{2+} binding curves of ScTnC F27W (n = 8), McTnC F27W (n = 8), and DVLG ScTnC F27W (n = 8) at 21 °C, pH 7.0. Data were normalized with respect to the maximal fluorescence of each Ca^{2+} titration and are presented as means ± SE. The curves were generated by fitting the data with the Hill equation.

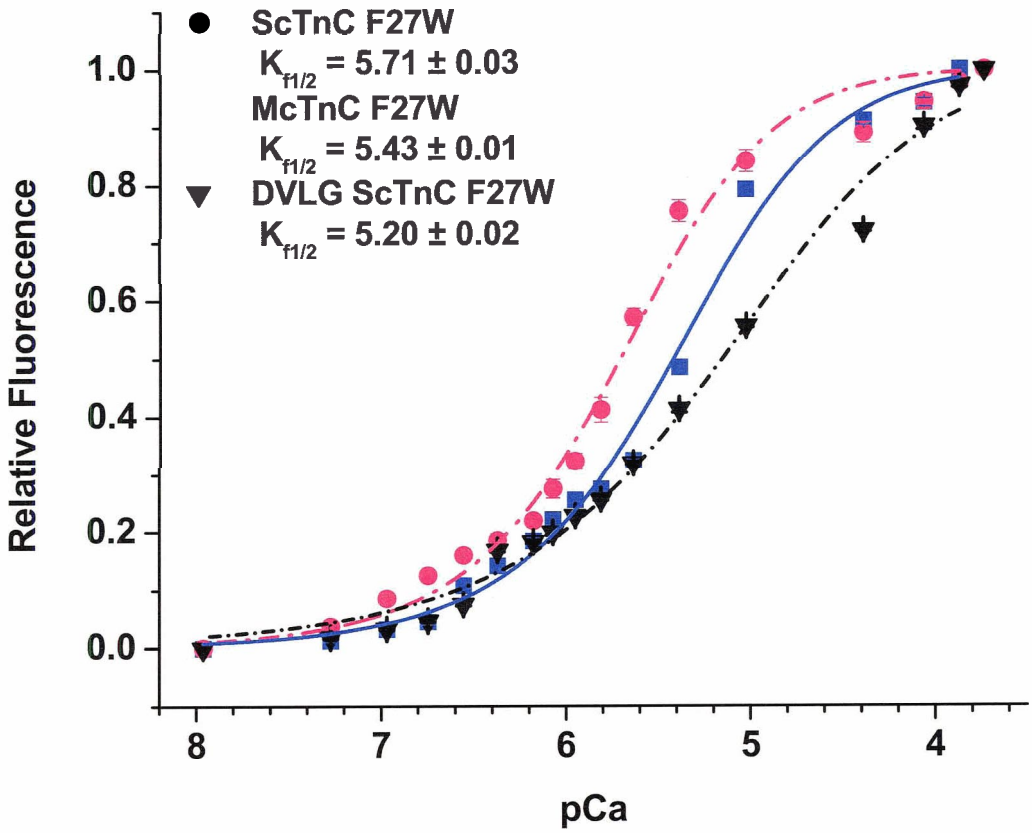

Figure 5-5. Steady state Ca^{2+} binding curves of RsTnC F27W (n = 8), chimeric TnC F27W (n = 8), and McTnC F27W (n = 8) at 21 °C, pH 7.0.
Data were normalized with respect to the maximal fluorescence of each Ca^{2+} titration and are presented as means ± SE. The curves were generated by fitting the data with the Hill equation.

** Not significantly different from each other (P > 0.05).

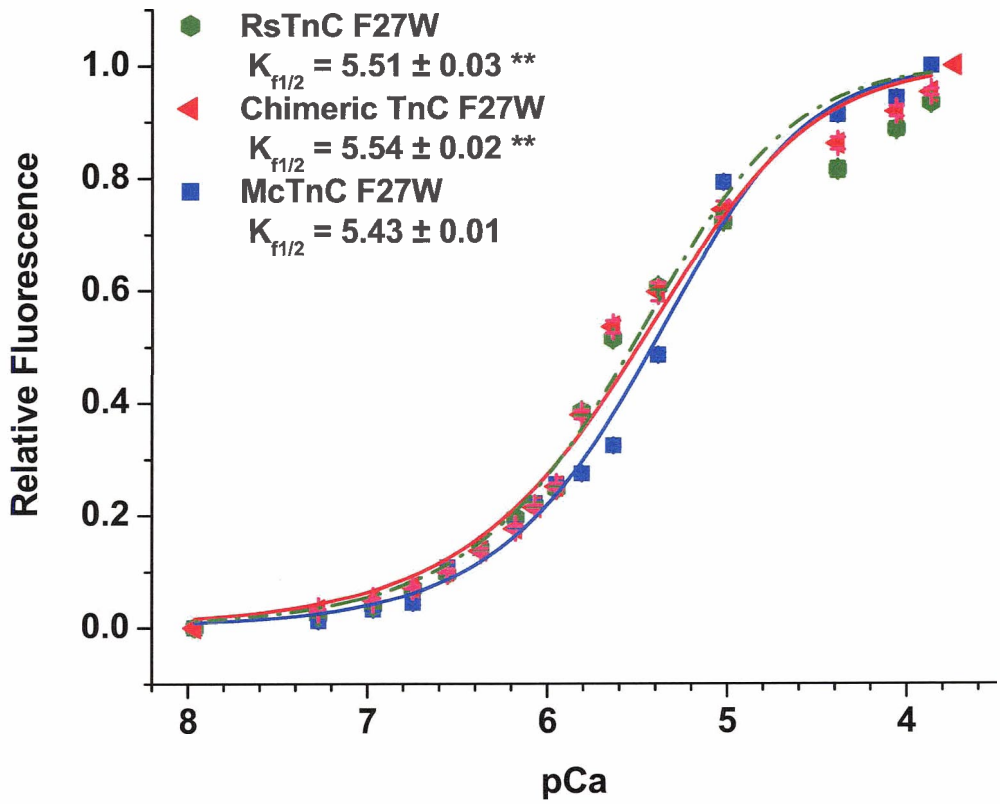

Although the molecular mechanism of cooperativity is not clearly understood, the Hill coefficient is often used to describe the cooperativity of Ca^{2+} binding to a single molecule with multiple binding sites or of Ca^{2+} activated tension in a functioning myofibril. A coefficient of 1.0 indicates completely independent binding regardless of the number of bound ligands. A number > 1.0 indicates positive cooperativity whereas a number < 1.0 indicates negative cooperativity.

Since cTnC contains only one Ca^{2+} activating site, cooperativity is unlikely. The Hill coefficients of these proteins as summarized in Table 5-1 were used solely as a parameter for curve fitting. The Hill coefficients for RsTnC and Chimeric TnC with two Ca^{2+} activating sites are 0.86 and 0.93, respectively indicates a lack of cooperativity between the first and second EF-hands. However, Pearlstone's group has shown that Hill coefficient derived from Ca^{2+} titration curves, as done in these experiments, are not reliable measurements of cooperativity (*68*).

Table 5-1. Summary of the Hill coefficients for various TnC and mutants *in vitro*.

Protein (n = 8)	Hill coefficient
McTnC F27W	0.96 ± 0.01
NIQD McTnC F27W	0.96 ± 0.01
L29Q McTnC F27W	0.98 ± 0.02
ScTnC F27W	1.04 ± 0.06
DVLG ScTnC F27W	0.75 ± 0.01
RsTnC F27W	0.86 ± 0.03
Chimeric TnC F27W	0.93 ± 0.03

5.2 Ca^{2+} binding kinetics of TnC F27W constructs

The Ca^{2+} dissociation rates from the regulatory domain of ScTnC F27W, McTnC F27W and the NIQD and L29Q mutants were determined using fluorescence stopped-flow measurements. The EGTA-induced decreases in tryptophan fluorescence were measured over time as Ca^{2+} was removed from the cTnC F27W proteins at 5 °C and 15 °C (Figures 5-6 and 5-7).

Figure 5-6. Rate of Ca^{2+} dissociation (k_{off}) from ScTnC F27W, McTnC F27W and its mutant at 5°C.
The traces were fitted with a single exponential after complete mixing (variance < 8×10^{-4}). The traces have been normalized and staggered for clarity.

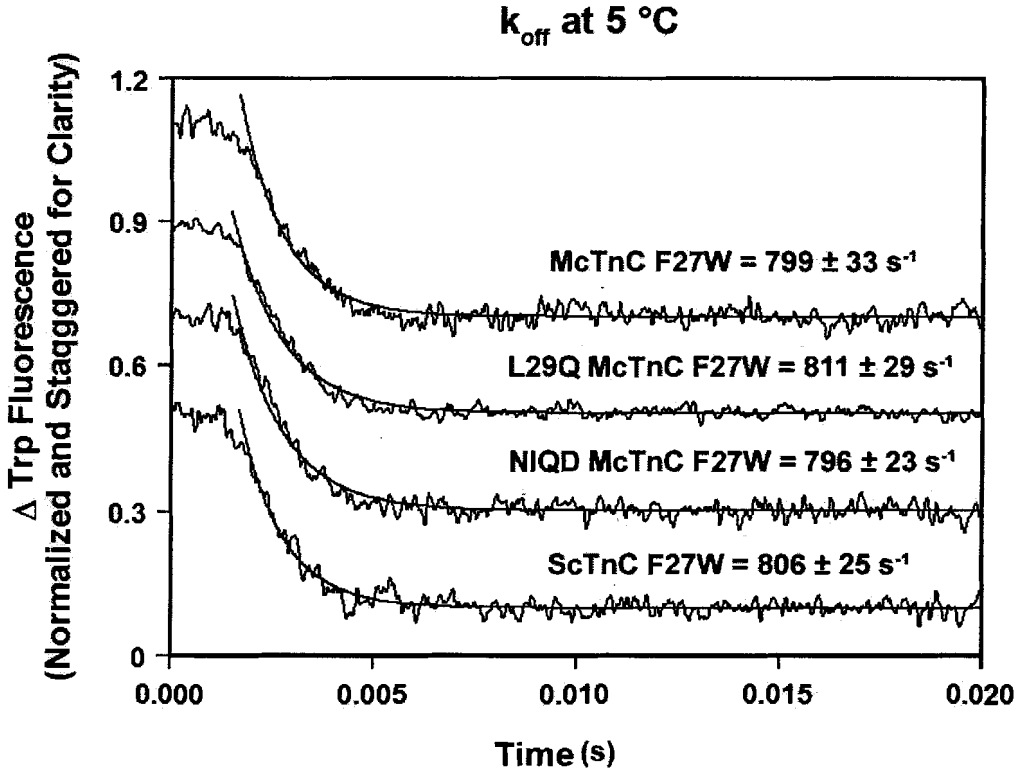

Figure 5-7. Rate of Ca^{2+} dissociation (k_{off}) from ScTnC F27W, McTnC F27W and mutant at 15°C.
The traces were fitted with a single exponential after complete mixing (variance < 8×10^{-4}). The traces have been normalized and staggered for clarity.

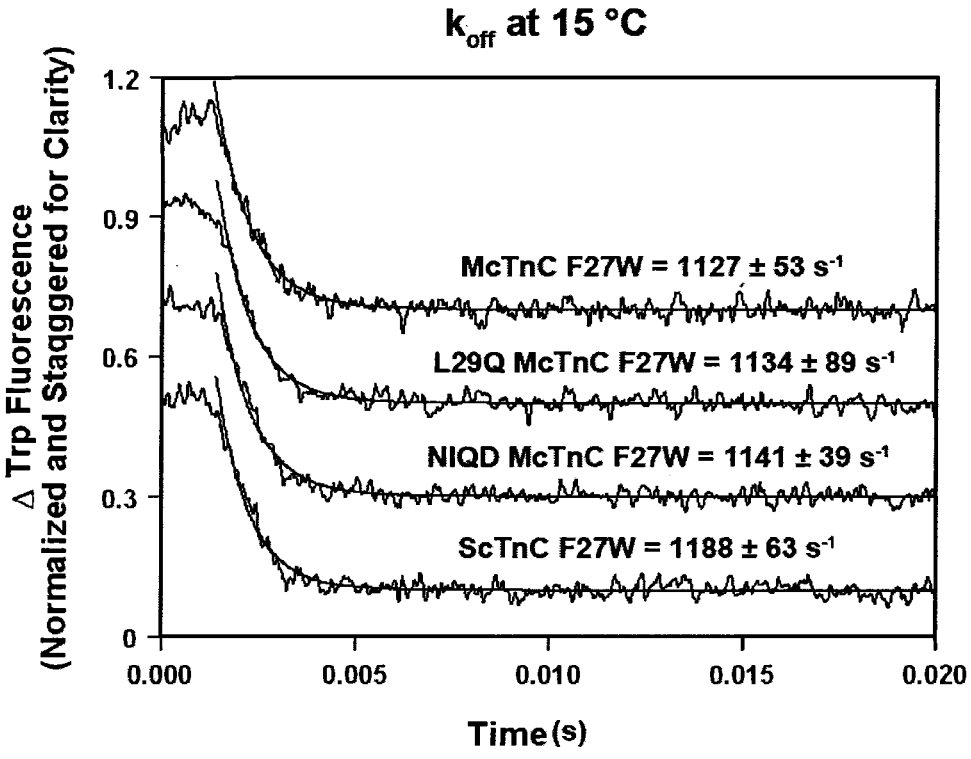

The k_{off} values of the TnC F27W proteins ranged from 796 ± 23 s^{-1} to 811 ± 29 s^{-1} and 1134 ± 89 s^{-1} to 1188 ± 63 s^{-1} at 5 °C and 15 °C, respectively. The sequence differences between McTnC and ScTnC and the residues substitution in McTnC did not greatly affect the k_{off} of Ca^{2+} binding. These k_{off} values at the two different temperatures allowed us to calculate the temperature coefficient Q_{10} which is defined as the change in the rate of k_{off} as a result of a change in temperature by 10 °C. The Q_{10} of the proteins ranged from 1.40 ± 0.01 to 1.47 ± 0.09 and are summarized in Table 5-2 along with the k_{off} values at 5 °C and 15 °C.

Table 5-2: Summary of k_{off} at 5 °C and 15 °C and temperature coefficient Q_{10} for ScTnC F27W, McTnC F27W and its mutant in the presence of 3 mM Mg^{2+}.

Protein	k_{off} (s^{-1}) at 15 °C	k_{off} (s^{-1}) at 5 °C	Q_{10} Based on k_{off}
McTnC F27W	1127 ± 53	799 ± 33	1.41 ± 0.08
L29Q McTnC F27W	1134 ± 89	811 ± 29	1.40 ± 0.1
NIQD McTnC F27W	1141 ± 39	796 ± 23	1.43 ± 0.06
ScTnC F27W	1188 ± 63	806 ± 25	1.47 ± 0.09

Since the Q_{10} is based on the relatively constant k_{off} values, it is not surprising to observe only a small variation in the Q_{10} of various mutants. Because the Ca^{2+} k_{off} is too fast for experimental measurements of Ca^{2+} k_{on}, this was estimated by exposing the cTnC F27W proteins to various ACTs of increasing amplitude and duration at 15 °C. The experiments were carried out in the presence of 3 mM Mg^{2+} to ensure complete occupation of the C-terminus cTnC F27W by Mg^{2+}. Because of the competitive binding of Mg^{2+} to the C-terminus cTnC, the simulations of the experimental data indicates true Ca^{2+} k_{on} (*15*). At the beginning of the experiment, successively increased concentrations of Ca^{2+} at 10 μM, 50 μM, 200 μM, and 5000 μM were mixed with an equal amount of 2 μM McTnC F27W, L29Q McTnC F27W, NIQD McTnC F27W, or ScTnC F27W protein with 1 mM EGTA. As the Ca^{2+} is subsequently chelated by EGTA and removed from the cTnC F27W proteins, the fluorescence decay is recorded. These experimental data (Figures 5-8 to 5-11) were reported as the time course of Ca^{2+} binding and subsequent dissociation from the activation site of cTnC F27W over time subjected to different ACTs. The Ca^{2+} k_{on} values could then be estimated because it is directly related to the percentage transient occupancy of Ca^{2+} bound to the cTnC. Each individual ACTs trace was simulated using the program KSIM as described in section 4.10. The derived k_{on} varied from $1.0 \pm 0.1 \times 10^{-8}$ $M^{-1}s^{-1}$to $2.1 \pm 0.2 \times 10^{-8}$ $M^{-1}s^{-1}$ at 15 °C and is summarized in Table 5-3 along with the calculated K_d.. The K_d which indicates the strength of binding between Ca^{2+} and TnC and how easy it is to separate the two was calculated using the equation $K_d = k_{off} / k_{on}$. Hence, the smaller the K_d, the stronger the binding between Ca^{2+} and TnC implying a higher Ca^{2+} affinity. The Ca^{2+} affinity data from the Ca^{2+} titration experiments and exposure to ACTs were consistent demonstrating a ~ 2-fold higher

affinity in ScTnC F27W and NIQD McTnC F27W and ~ 37% higher affinity in L29Q F27W when compared to McTnC F27W.

Table 5-3. Summary of k_{off}, simulated k_{on}, and calculated K_d for ScTnC F27W, McTnC F27W and its mutant at 15 °C in the presence of 3 mM Mg^{2+}.

Protein	k_{off} (s^{-1})	Simulated k_{on} ($\times 10^8$ M^{-1} s^{-1})	Calculated K_d (μM)
McTnC F27W	1127 ± 53	1.0 ± 0.1	11.0 ± 1.0
L29Q McTnC F27W	1134 ± 89	1.5 ± 0.2	8.0 ± 1.0
NIQD McTnC F27W	1141 ± 39	2.0 ± 0.2	5.7 ± 0.6
ScTnC F27W	1188 ± 63	2.1 ± 0.2	5.7 ± 0.6

Figure 5-8. Percentage of Ca^{2+} occupancy of McTnC F27W during artificial Ca^{2+} transients of different amplitude and duration at 15 °C.

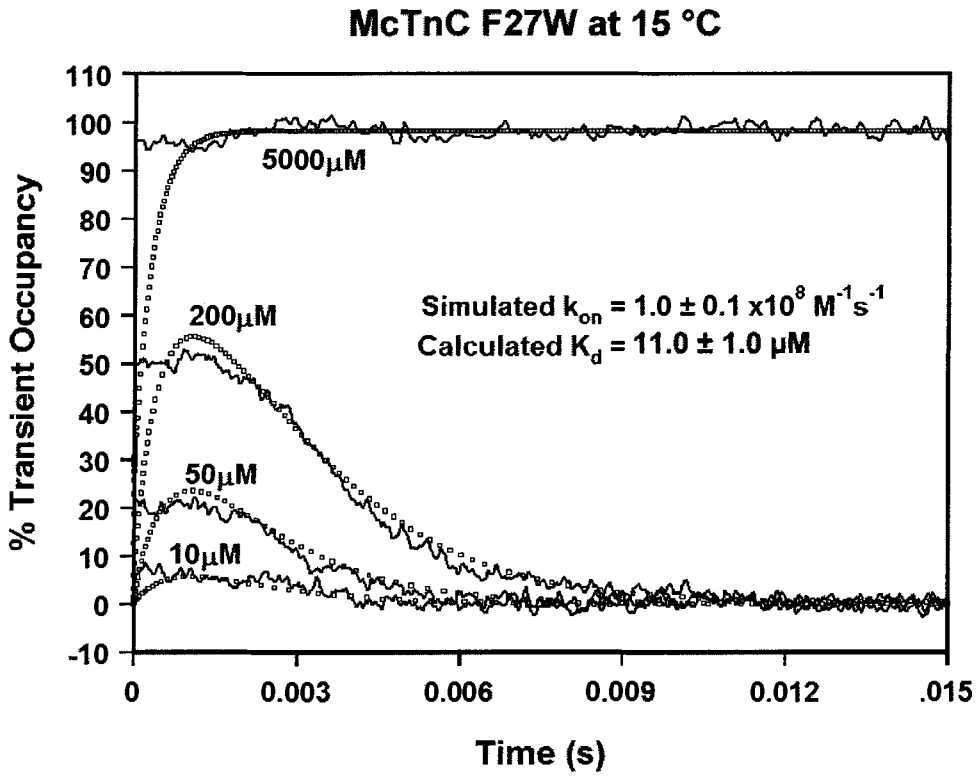

Figure 5-9. Percentage of Ca^{2+} occupancy of L29Q McTnC F27W during artificial Ca^{2+} transients of different amplitude and duration at 15 °C.

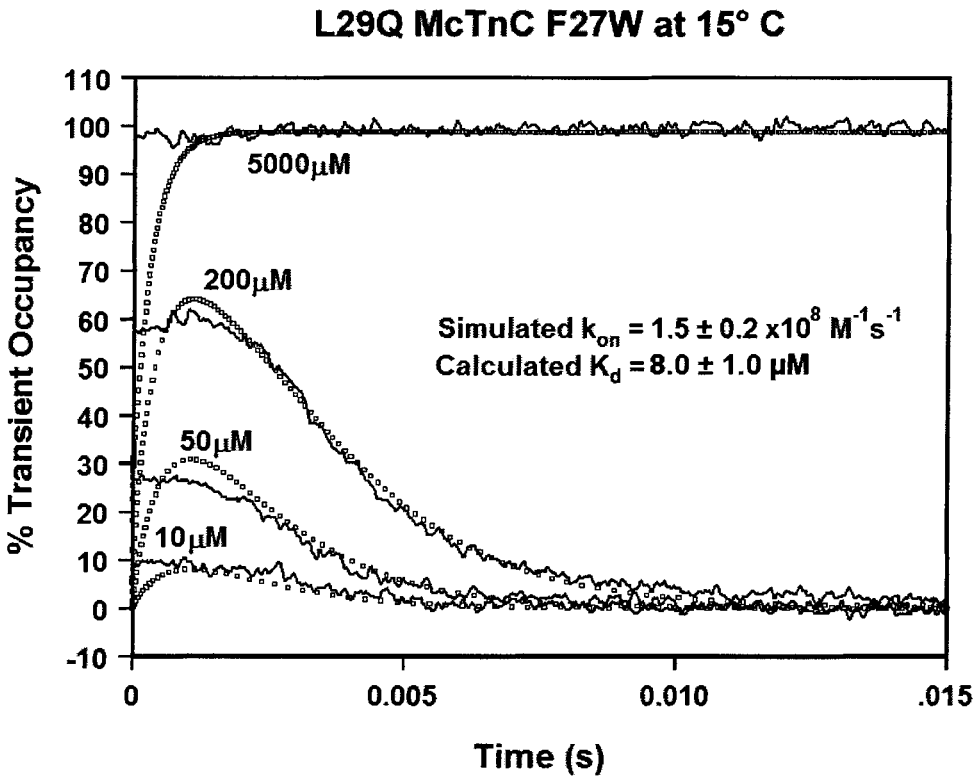

Figure 5-10. Percentage of Ca^{2+} occupancy of NIQD McTnC F27W during artificial Ca^{2+} transients of different amplitude and duration at 15 °C.

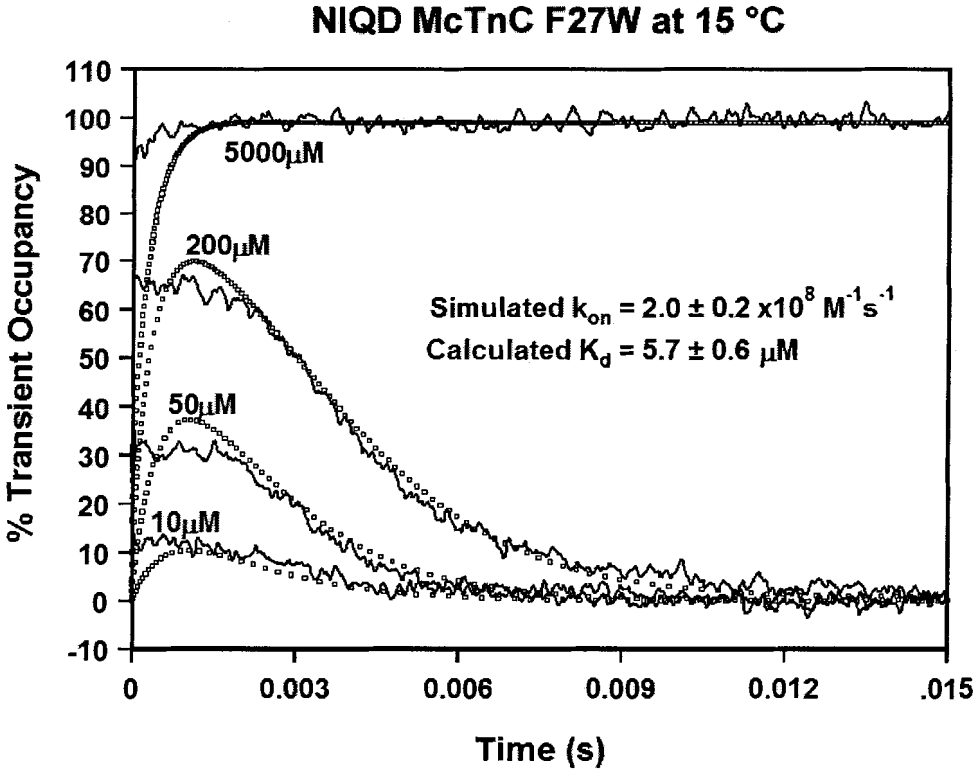

Figure 5-11. Percentage of Ca^{2+} occupancy of ScTnC F27W during artificial Ca^{2+} transients of different amplitude and duration at 15 °C.

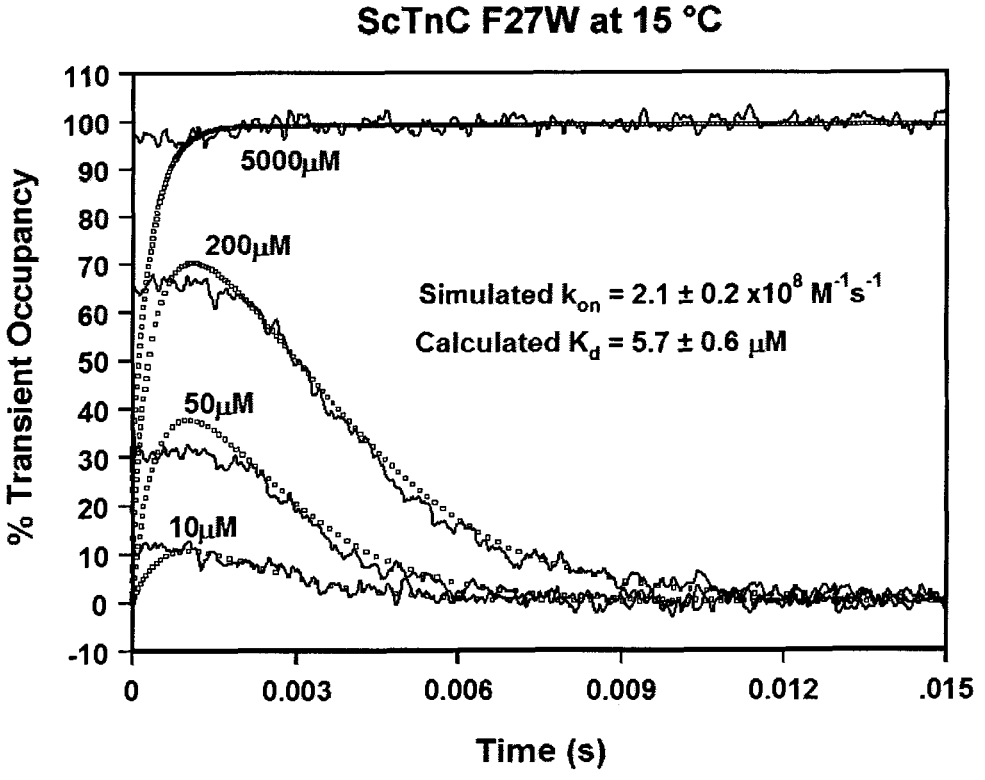

5.3 Force-pCa measurement in single cardiac myocytes

Prior to extraction of endogenous murine mcTnC, the average F_{max} generated at pCa 4.5 by a single myocyte was 1.21 ± 0.12 mg, and this value was taken as the maximum force-generating capacity of the myocyte. After extraction, the force generated was only 11.2 ± 2.0% of F_{max} indicating an effective extraction (Figure 5-12). On reconstitution with various TnC molecules, myocytes that showed altered sarcomere pattern or did not achieve 80% of the original F_{max} after the extraction/reconstitution protocol were discarded. Examples of successful reconstitution are McTnC and NIQD McTnC with Ca^{2+} generated force 82.7 ± 2.3% and 80.8 ± 2.0% respectively of F_{max}. Although the force produced by the reconstituted myocytes were statistically less ($P < 0.05$) than that produced by the pre-extracted myocytes, this amount of force recovery indicates successful reconstitution. These results also indicate that there was no obvious difference in how McTnC and NIQC McTnC were incorporated into the myocytes. Because the data from each experiment were normalized to unity (with 1 being force produced at pCa 4.5) before fitting the data with the Hill equation, it was possible for relative force-pCa comparison between treatment groups.

Figure 5-12. Representative time-based digital recordings of force generated by cardiomyocyte before mcTnC extraction, after extraction, and after McTnC reconstitution.
The first force break in recording represents the incubation period in extraction solution, and the second recording break represents the incubation period in a relaxing solution containing mcTnC.

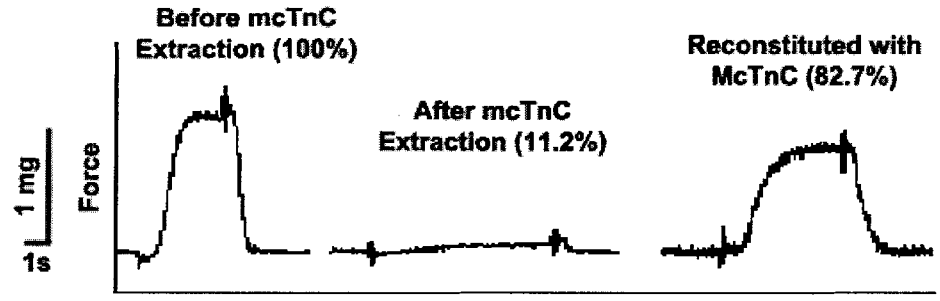

Similar cTnC extraction and reconstitution rates were reported by Martyn and Gordon (*69*). After extraction of the endogenous cTnC, the myocytes become relatively insensitive to Ca^{2+}. Nevertheless, Ca^{2+} sensitivity of the preparation is restored after incubation in TnC solution indicating that the loss of Ca^{2+} sensitivity is due to the loss of functional TnC. In addition, Regnier's group (*70*) has shown that the preparation remains insensitive to Ca^{2+} after reconstitution with TnC that are unable to be activated by Ca^{2+}.

Various attempts were made to reconstitute ScTnC into the mouse cardiac myocytes; however, there was no force recovery, suggesting that the protein did not incorporate into the sarcomeres. The sequence difference in the C-terminus of McTnC and ScTnC may have affected how this protein incorporates into the sarcomere. Efforts were also made to replace endogenous ScTnC with McTnC in trout cardiac myocytes, but it was not possible to effectively monitor sarcomere length in these preparations.

Exposure of the myocytes containing either endogenous mcTnC, reconstituted TnC to increasing Ca^{2+} concentration caused an increase in the amount of force generation that reached a maximum at pCa 4.5 (Figure 5-13 to 5-15). This shows that force generation is Ca^{2+} sensitive in these myocytes. The Ca^{2+} titration curve of mcTnC and McTnC (Figure 5-13) are virtually superimposable with a $P > 0.05$ indicating not significantly different $K_{F1/2}$ (pCa at half-maximal force), an indicator of Ca^{2+} sensitivity which represents the binding event of Ca^{2+} ion to the activating site of TnC *in situ*. This result provides evidence that the extraction/reconstitution protocol had no affect on the Ca^{2+} sensitivity of force generation and the sequence differences between mcTnC and McTnC did not substantively affect the Ca^{2+} sensitivity of force generation.

The force-pCa curves of NIQD McTnC and L29Q McTnC (Figure 5-14) were left-shifted indicating an increase in Ca^{2+} sensitivity. NIQD McTnC and L29Q McTnC were found to be ~ 82% and ~ 38%, respectively more sensitive to Ca^{2+} to the cardiomyocytes containing either mcTnC or McTnC.

The N-terminus skeletal C-terminus cardiac chimeric TnC was successfully reconstituted into mouse cardiac myocytes (Figure 5-15). The Ca^{2+} affinity of the chimeric TnC was significantly different from McTnC and this supports our hypothesis that it is the sequence difference in the C-terminus that affects how the protein is incorporated into the sarcomere. The force-pCa curve generated by the chimeric TnC was left-shifted indicating a ~ 45% increase in Ca^{2+} sensitivity compared to that of mcTnC or McTnC.

Figure 5-13. Ca^{2+} titration of steady-state force generation in single, skinned, mouse cardiac myocyte containing McTnC (n = 8) and endogenous (preextracted) mcTnC (n = 8) at 15 °C, pH 7.0.
Data were normalized with respect to the maximal force generated during each Ca^{2+} titration and are presented as means ± SE. The curves were generated by fitting the data with the Hill equation.

† Not significantly different from each other (P > 0.05).

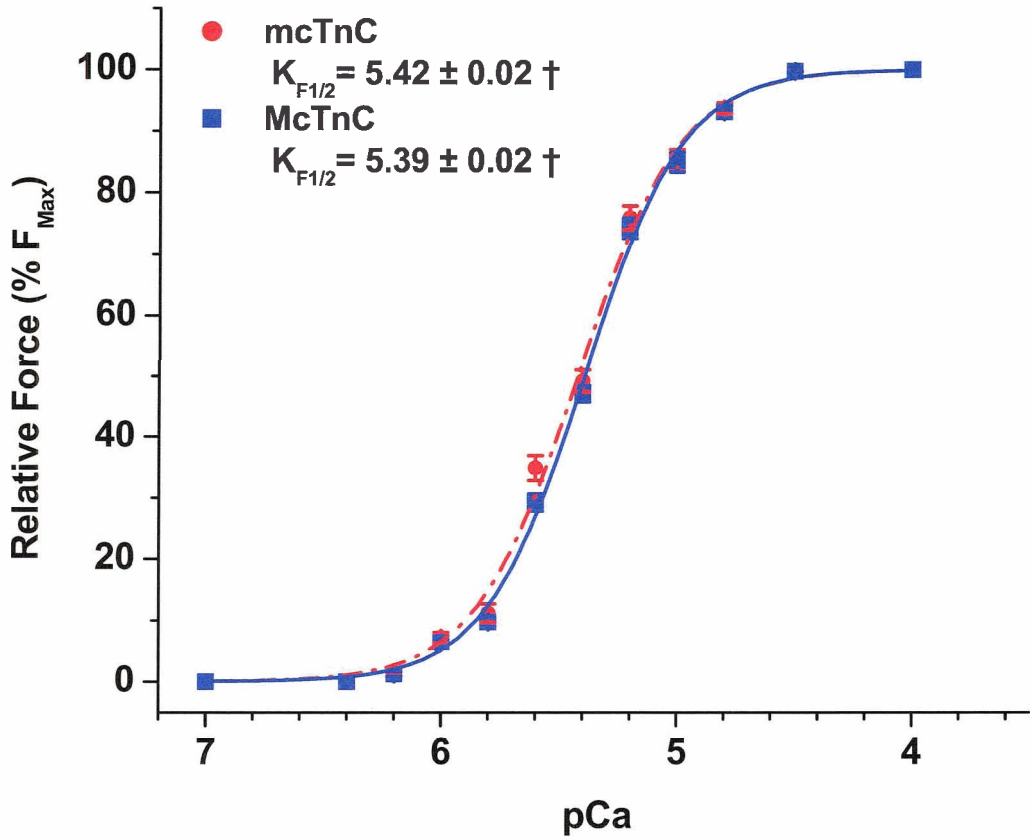

Figure 5-14. Ca^{2+} titration of steady-state force generation in single, skinned, mouse cardiac myocyte containing NIQD McTnC (n = 7), L29Q McTnC (n = 6), McTnC (n = 8), and endogenous (preextracted) mcTnC (n = 8) at 15 °C, pH 7.0.
Data were normalized with respect to the maximal force generated during each Ca^{2+} titration and are presented as means ± SE. The curves were generated by fitting the data with the Hill equation.

† Not significantly different from each other (P > 0.05).

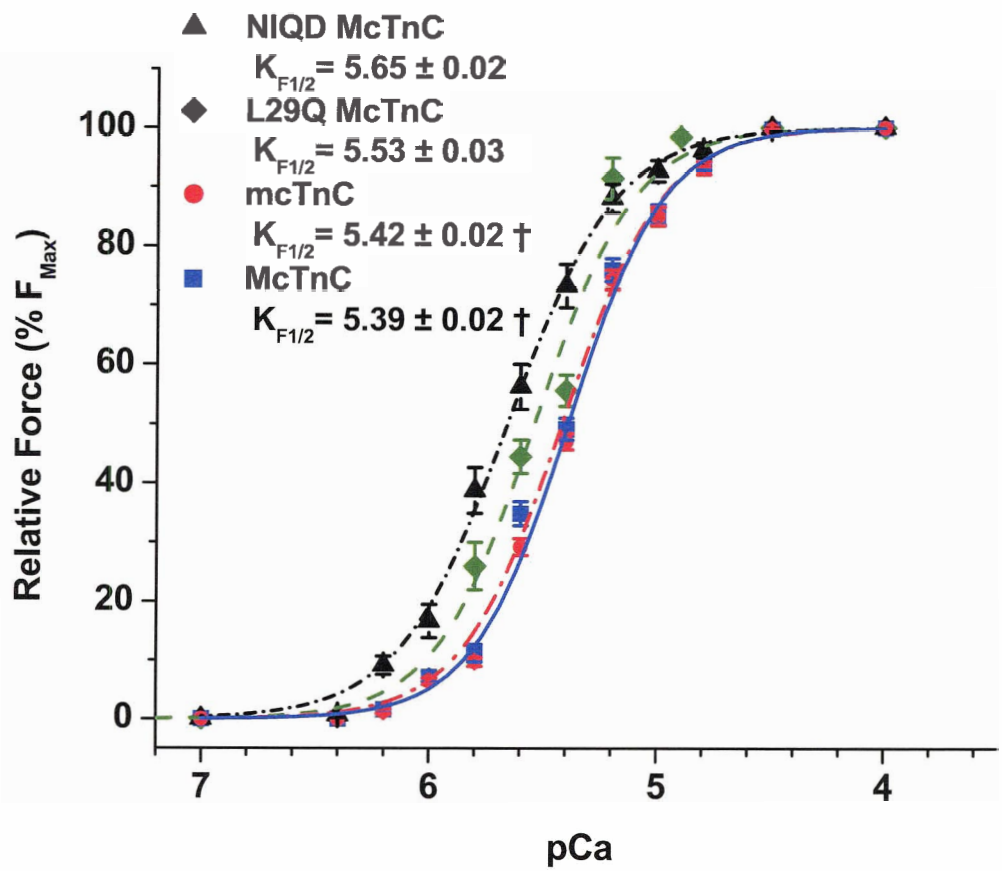

Figure 5-15. Ca^{2+} titration of steady-state force generation in single, skinned, mouse cardiac myocyte containing chimeric TnC (n = 5), endogenous (preextracted) mcTnC (n = 8), and McTnC (n = 8) at 15 °C, pH 7.0. Data were normalized with respect to the maximal force generated during each Ca^{2+} titration and are presented as means ± SE. The curves were generated by fitting the data with the Hill equation.

† Not significantly different from each other (P > 0.05).

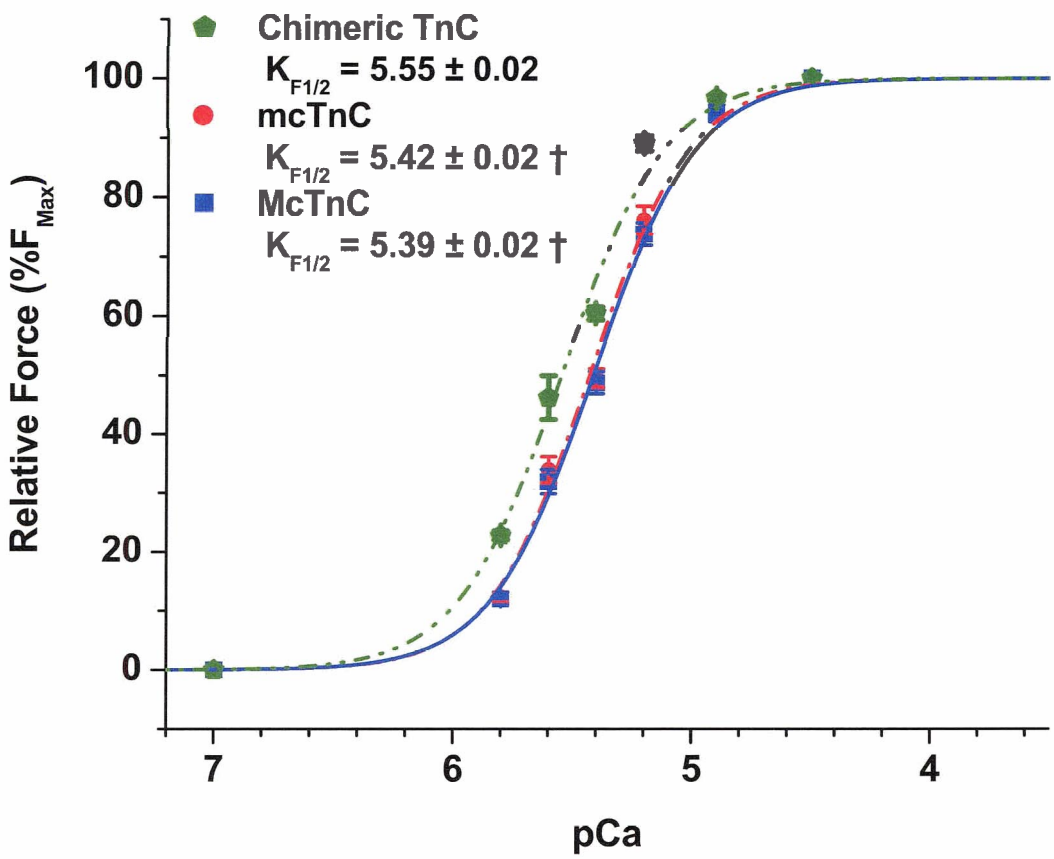

The Hill coefficients of *in situ* experiments, which provide a measurement of the degree of cooperativity between units of the thin filament, are summarized in Table 5-4. The Hill coefficients of the various TnC were not significantly different from each other ranging from 2.11 ± 0.07 to 2.18 ± 0.02 and the > 1 value indicates positive cooperativity. The are four possible sources of cooperativity including: 1) coupling between the two N-terminus regulatory sites in sTnC; 2) coupling between Ca^{2+} binding sites on the thin filament; 3) the effect of strongly bound cross-bridges which acts through tropomyosin and troponin to increase Ca^{2+} binding to the thin filament; and 4) strongly bound cross-bridge induced activation of the thin filament (*6*). The comparable Hill coefficients suggest that the sequence difference between the wild type McTnC, mutant McTnC, and chimeric TnC did not affect the degree of cooperativity.

Table 5-4. Summary of the Hill coefficients for various TnC and mutants *in situ*.

Protein	$K_{F1/2}$ (n)	Hill coefficient
McTnC	5.39 ± 0.01 (8)	2.13 ± 0.02
NIQD McTnC	5.65 ± 0.02 (7)	2.17 ± 0.17
L29Q McTnC	5.53 ± 0.03 (6)	2.13 ± 0.04
Chimeric TnC	5.55 ± 0.02 (5)	2.11 ± 0.07
mcTnC	5.42 ± 0.02 (8)	2.18 ± 0.02

5.4 Pioneering 7ZW experiments

The effect of 7ZW at residue 27 of TnC was also tested. The special fluorescence properties of this unnatural amino may become a valuable tool in future research. 7ZW was engineered into TnC and its mutants as a reporter in the measurement of Ca^{2+} activation *in vitro*. By comparing the results of the tryptophan and 7ZW reporters *in vitro*, we were able to determine the influence of the two probes on the Ca^{2+} binding of TnC. The overall trends of the Ca^{2+} titration curves of the 7ZW TnC (Figure 5-16) are similar to that of F27W TnC with an overall ~ 48% decrease in Ca^{2+} affinity. Studies by Valencia et al (*54*) also observed a comparable decrease in Ca^{2+} affinity in 7ZW TnC proteins. The F27ZW TnC mutants demonstrate similar changes in Ca^{2+} affinity compared to the F27W TnC mutants. When compared to McTnC F27ZW, the NIQD McTnC F27ZW and chimeric TnC F27ZW showed ~ 93% and ~ 35% increase in Ca^{2+} affinity, respectively. In conclusion, 7ZW does affect the Ca^{2+} affinity of the protein, as shown in the differences in $K_{f1/2}$ values, but the affect is uniform in all mutants.

The McTnC F27ZW was reconstituted into single skinned cardiomyocytes to determine the efficacy of use of 7ZW TnC proteins *in situ*. The Ca^{2+} titration curve of McTnC F27ZW (Figure 5-17)was similar to that of mcTnC and McTnC with a right shift indicating ~ 30% decrease in Ca^{2+} sensitivity. This provides preliminary evidence that 7ZW TnC proteins report Ca^{2+} binding in a similar manner as TnC proteins *in situ* and the possibility of monitoring Ca^{2+} binding to TnC and the force generation simultaneously, which has not been achieved before.

Figure 5-16. Steady state Ca^{2+} binding curves of NIQD McTnC F27ZW (n = 8), chimeric TnC F27ZW (n = 8), and McTnC F27ZW (n = 8) at 15 °C, pH 7.0. Data were normalized with respect to the maximal force generated during each Ca^{2+} titration and are presented as means ± SE. The curves were generated by fitting the data with the Hill equation.

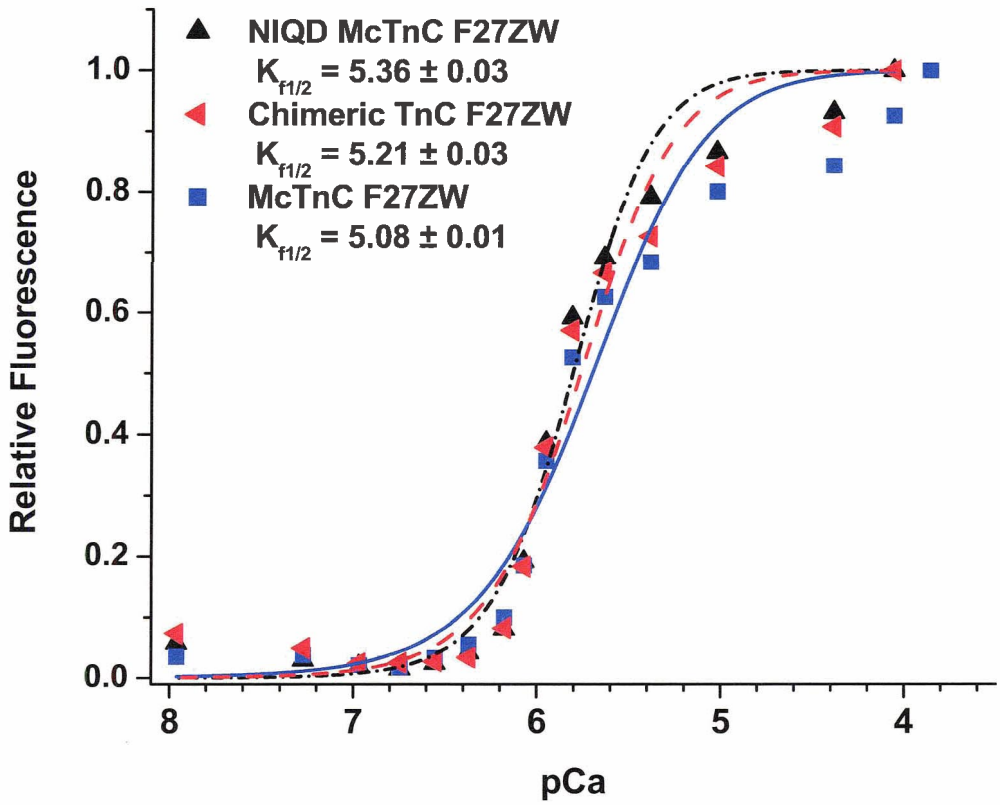

Figure 5-17. Ca^{2+} titration of steady-state force generation in single, skinned, mouse cardiac myocyte containing endogenous (preextracted) mcTnC (n = 8), McTnC (n = 8), and McTnC F27ZW (n = 2) at 15 °C, pH 7.0. Statistical analysis was not performed on McTnC F27ZW due to the small sample number. Data were normalized with respect to the maximal force generated during each Ca^{2+} titration and are presented as means ± SE. The curves were generated by fitting the data with the Hill equation.

† Not significantly different from each other (P > 0.05).

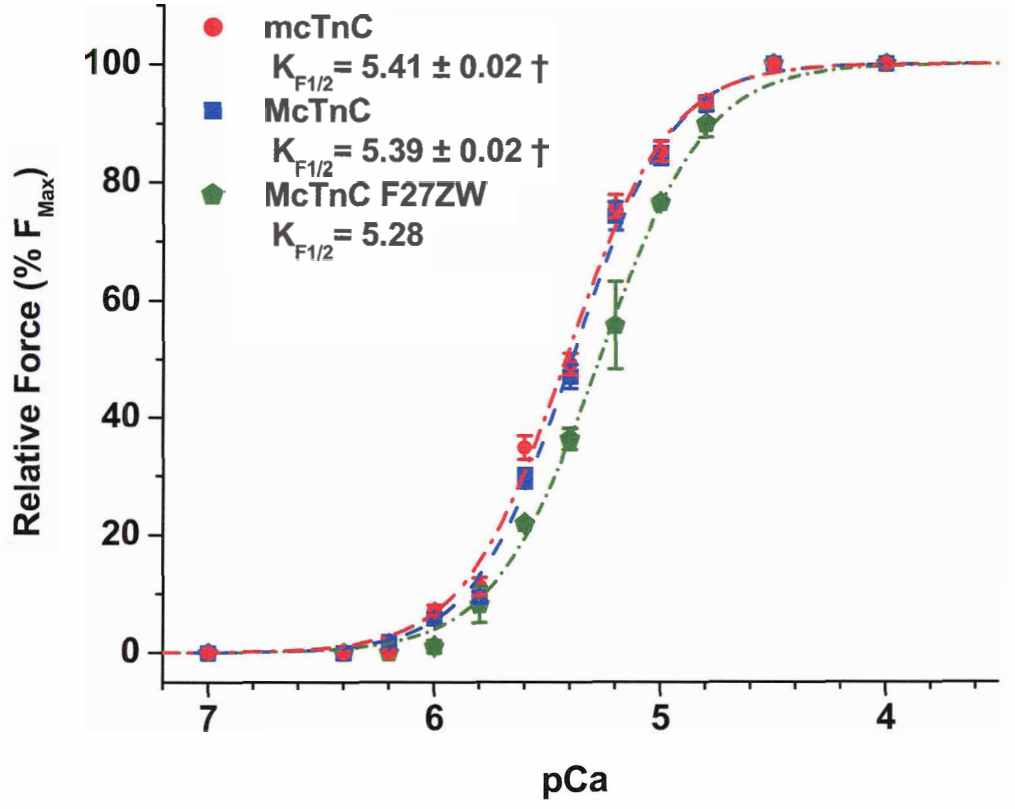

6. GENERAL DISCUSSION

6.1 Ca^{2+} affinity measurements

Substitutions of residues D2N, V28I, L29Q, and Q30D in truncated and full length McTnC have demonstrated an increase in Ca^{2+} affinity by ~ 2 fold to an equivalent of ScTnC. A reciprocal of these substitutions in ScTnC also resulted in ~ 41% decrease in Ca^{2+} affinity. These results demonstrate these four amino acid substitutions of ScTnC are at least largely responsible for the comparatively high Ca^{2+} affinity of trout cardiac myocytes. The difference in Ca^{2+} affinity was retained in the full length cTnC proteins compared to the truncated cTnC indicating that it is the difference in the N-terminus of cTnC that is responsible for the difference in function and Ca^{2+} activation. This was further verified by the skeletal-cardiac chimeric TnC possessing a similar Ca^{2+} affinity to RsTnC which was significantly different from McTnC (Figure 5-5).

The Ca^{2+} affinity and sensitivity of the FHC related mutation L29Q McTnC was increased by ~ 32% and ~ 38%, respectively compared to McTnC. Since the above residues are located outside the regulatory site II, the increase in Ca^{2+} affinity must be the result of the altered Ca^{2+} binding ability in site II by an allosteric effect. Nuclear magnetic resonance (NMR) solution studies by Spyracopoulos' group (*71*) have demonstrated that sites I and II of cTnC are structurally linked; hence, it is not surprising that sequence difference in site I can affect the structure of site II. Furthermore, the NMR spectroscopy revealed different structures of McNTnC and ScNTnC at 30 °C illustrating

that the sequence differences between the two in site I can in turn affect the structural organization of site II and ultimately its Ca^{2+} binding ability (*46*).

During Ca^{2+} activation of cTnC, helices B and C move away from helices N, A, and D exposing a hydrophobic patch that allows for the interaction of N-terminus cTnC and C-terminus cTnI which releases the inhibition effect of cTnI and initiates a cascade of events that leads to muscle contraction (*25*). Preceding studies have suggested that mutations which stabilize the interaction of helices B and C with helices N, A, and D in the apo state through disulfide bond or salt bridge formation would decrease the Ca^{2+} affinity of the regulatory domain (*72, 73*). Alternatively, an increase in Ca^{2+} affinity is observed in mutations that shift the TnC equilibrium towards the Ca^{2+} bound state by reducing the amount of hydrophobic patch exposure when Ca^{2+} is bound (*74*). Hence, Ca^{2+} affinity is directly related to the amount of energy associated with the conformational change in sites I and II of TnC.

A study by Sia et al (*75*) has shown that the non polar, hydrophobic leucine residue 29 in cTnC plays an important role in the integrity of helix A and therefore the non-functioning site I. The destabilization of helix A by a polar, hydrophilic L29Q substitution might indirectly affect the Ca^{2+} binding properties of the adjacent site II in cTnC (*76*) resulting in an increased Ca^{2+} affinity. A study by Tikunova and Davis (*64*) demonstrated the single substitution of glutamine in place of hydrophobic residues 20, 44, 45, 48, and 81 resulted in a large increase in Ca^{2+} affinity in the N-terminus TnC. They postulated that the glutamine substitution reduces the hydrophobic contact between helices B and C with N, A, and D in the apo state, thereby destabilizing the protein and facilitating the opening of the TnC molecule during Ca^{2+} activation. This hypothesis was

however contrasted by the 3-D structure of the N-terminus McTnC where residue 29 is located on the surface of the molecule (*46*). The loss of a hydrophobic residue in that area should not affect the core stability of the molecule. However, it is possible that the L29Q substitution could have decreased the local protein stability by increasing the interaction between the cTnC protein and its solvent, mimicking the effects of cTnI binding which stabilizes the cTnC protein in the "open" conformation.

Functional evidence suggest ScTnC to be less stable with a greater molecular flexibility than McTnC as the former lost its tertiary structure and was perhaps denatured at 37 °C (*1*). Similar thermal denaturation and increased molecular flexibility in the protein have been observed in studies of other cold-adapted species (*77, 78*). This increase in flexibility has been suggested as a mechanism to cope with reduced chemical reaction rates induced by lower physiological temperatures. The amino acids substitutions responsible for the higher Ca^{2+} affinity in ScTnC could have increased the molecular flexibility and decreased the compactness of either a selected area or the overall protein structure, in turn decreasing the energy of Ca^{2+} activation resulting in an increased Ca^{2+} affinity.

The tryptophan or 7-azatryptophan was inserted at residue 27 as a fluorescence reporter to characterize the Ca^{2+} affinity and binding kinetics of various TnCs and their mutants. The possible effect of this mutation in TnC was negated as all the proteins characterized contained this mutation. The difference in Ca^{2+} affinity between the F27W and F27ZW TnC were almost identical, with F27ZW TnC proteins overall showing an ~ 48% decrease in Ca^{2+} affinity compared to F27W TnC. The same decrease in Ca^{2+} affinity between F27W and F27ZW TnC was observed by Valencia et al (*54*).

6.2 Ca^{2+} binding properties

A combination of the stopped-flow and ACTs technique was used on ScTnC F27W, McTnC F27W and its NIQD and L29Q mutant to determine the Ca^{2+} k_{off} and k_{on}, respectively. The 1.6 ms dead time of the stopped-flow apparatus make it impossible to directly measure the k_{on} because most of the reaction occurred during that time frame. The stopped-flow and ACTs data were obtained in the presence of 3 mM Mg^{2+} to ensure complete Mg^{2+} occupation of the C-terminus cTnC because a previous study (*15*) found it impossible to simulate the obtained ACTs data due to interference of the C-terminus cTnC which arise from interdomain interactions. Although the solution used contained Mg^{2+}, these data still estimate true Ca^{2+} k_{off} and k_{on} independent of [Mg^{2+}] due to competitive Mg^{2+} binding to site II cTnC. Similar Ca^{2+} k_{off} values have been reported in fluorescence stopped-flow measurements taken with or without Mg^{2+} (*15*)

There were very little fluctuations in the k_{off} of the cTnC F27W proteins within the 5 °C and 15 °C temperature groups. It is no surprise that the relatively constant k_{off} lead to small variations in its Q_{10} ranging from 1.40 ± 0.01 to 1.47 ± 0.09. Although small, the Q_{10} value signifies ~ 40% to 47% increase in reaction rate when the temperature was increased by 10 °C and vice versa. A parallel relationship was observed between the k_{on} and the calculated K_d. The k_{on} doubled from $1.0 \pm 0.1 \times 10^{-8}$ $M^{-1}s^{-1}$ to $2.1 \pm 0.2 \times 10^{-8}$ $M^{-1}s^{-1}$ between McTnC and ScTnC at 15°C as the binding affinity between Ca^{2+} and cTnC increased by ~ 2 fold as reflected in the K_d. The increase in Ca^{2+} affinity of these cTnC mutants was solely due to an increase in Ca^{2+} association rates.

Since any changes in k_{on} could potentially affect the equilibrium of the protein in the apo state (*15*), the increase in k_{on} can be interpreted as a decrease in the energy associated with conformational changes of the protein. The data obtained are coherent with the idea that the higher Ca^{2+} affinity and sensitivity of ScTnC is a result of a decreased energy of activation. In spite of that, structural analyses such as X-ray crystallography and NMR spectroscopy are required in future studies to determine the mechanism by which those four N-terminus amino acid residues substitution can have such a dramatic impact on cardiac contractility.

The tryptophan was inserted at residue 27 as a fluorescence reporter to enable measurements of Ca^{2+} exchanges in the regulatory site of cTnC. Again, the effect of this mutation in TnC was negated as all the proteins characterized contained this mutation. Tikunova and Davis (*15*) confirmed that the F27W mutation truly reports Ca^{2+} k_{off} from the regulatory site of cTnC as the k_{off} measured using the fluorescence Ca^{2+} chelator Quin-2 yielded nearly identical rates from the EGTA-induced tryptophan changes.

6.3 Effects of TnC mutants on cardiomyocyte contractility

The force-pCa curves of the two McTnC mutants, NIQD and L29Q, and chimeric TnC were all left shifted from mcTnC and McTnC indicating an increased Ca^{2+} sensitivity. The increase in Ca^{2+} sensitivity between the McTnC mutants and McTnC were similar to the increase in Ca^{2+}affinity determined using the F27W mutation in the fluorescence studies. However, when the chimeric TnC was compared to McTnC, there was a ~ 45% increase in Ca^{2+} sensitivity which was greater than the ~ 28% increase in

Ca^{2+} affinity *in vitro*. This greater increase in Ca^{2+} sensitivity was not due to the length dependence of TnC Ca^{2+} binding as the single skinned cardiomyocytes preparation allows for effective control of the sacromere length to 2.1 μm while the cell was contracting. This difference may be a result of the allosteric interaction of chimeric TnC with other proteins on the thin filament. The N-terminus of McTnC and RsTnC contains 25 out of 87 amino acids differences with ~ 68% identity (Figure 1-4) and these sequence differences may have affected how the chimeric TnC interacts with TnI and TnT which can directly affect the Ca^{2+} sensitivity.

The TnC fibre replacements were completed at 15 °C, pH 7.0, whereas the fluorescence measurements were completed at 21 °C, pH 7.0. The 15 °C temperature was used to maintain the functional integrity of the cardiomyocytes. The difference at which these studies were completed should not affect the relative difference in Ca^{2+} affinity between the various TnC isoforms as Gillis et al (*1*) have shown that the difference in Ca^{2+} affinity between McTnC F27W and ScTnC F27W are maintained over a range of temperatures and pHs. Because the temperature and pH are held constant in each study, the difference in protein sequence is the only factor that is responsible for any differences in Ca^{2+} affinity and sensitivity. Wild-type TnC lacking the F27W mutation was used to measure the force tension generation in cardiomyocytes in fibre replacement as opposed to the *in vitro* studies which measure fluorescence changes.

6.4 The use of 7ZW in future research

The overall trends of the Ca^{2+} titration curves of the 7ZW TnC are similar to that of F27W TnC with an overall ~ 48% decrease in fluorescence which might have been a result of the 7ZW reporter. This demonstrates that the F27ZW mutation does affect the

Ca^{2+} affinity of the protein, but the affect was uniform in all mutants. The decreased Ca^{2+} affinity and sensitivity of the F27ZW mutants might have been a result of the bulkier indole side chain of the 7ZW reporter. The successful reconstitution of McTnC F27ZW into single skinned cardiomyocytes that produced a Ca^{2+} titration curve similar to that of McTnC with a ~ 30% decrease in Ca^{2+} sensitivity. The data provided preliminary evidence that 7ZW TnC proteins report Ca^{2+} binding in a similar manner as TnC proteins *in situ*. With the addition of a fluorescence monitor in future studies, it holds the possibility of monitoring Ca^{2+} binding to TnC and the force generation simultaneously, which has not been achieved before.

6.5 Summary

The Ca^{2+} sensitizing capabilities of the NIQD McTnC may represent a new tool in developing treatment modalities for heart failure without decreasing the rate of Ca^{2+} dissociation, which may lead to impaired relaxation, an undesirable effect of Ca^{2+} sensitizing agents. The L29Q McTnC substitution lead to increased Ca^{2+} affinity and sensitivity as a result of increased rate of Ca^{2+} association may provide groundwork explanation as to why this mutation is related to patients with familial hypertrophic cardiomyopathy (FHC). The regulatory role of the N-terminus TnC was reconfirmed by the identical Ca^{2+} affinity of the chimeric TnC with sTnC. The efficacy of use of the novel amino acid, 7-azatryptophan into TnC was verified in the *in vitro* and *in situ* studies. In conclusion, the studies in this thesis provided a better understanding of the structure function relationship of the cTnC molecule and lay the foundation for future studies.

LITERATURE CITED

(1) Gillis, T. E., Marshall, C. R., Xue, X. H., Borgford, T. J., and Tibbits, G. F. (2000) Ca^{2+} binding to cardiac troponin C: effects of temperature and pH on mammalian and salmonid isoforms. *Am J Physiol Regul Integr Comp Physiol 279*, R1707-15.

(2) Gillis, T. E., Moyes, C. D., and Tibbits, G. F. (2003) Sequence mutations in teleost cardiac troponin C that are permissive of high Ca^{2+} affinity of site II. *Am J Physiol Cell Physiol 284*, C1176-84.

(3) Fabiato, A. (1983) Calcium-induced release of calcium from the cardiac sarcoplasmic reticulum. *Am J Physiol 245*, C1-14.

(4) Bers, D. M. (2001) Excitation-contraction coupling and cardiac contractile force.

(5) Bers, D. M. (2002) Cardiac excitation-contraction coupling. *Nature 415*, 198-205.

(6) Gordon, A. M., Homsher, E., and Regnier, M. (2000) Regulation of contraction in striated muscle. *Physiol Rev 80*, 853-924.

(7) Gordon, A. M., Regnier, M., and Homsher, E. (2001) Skeletal and cardiac muscle contractile activation: tropomyosin "rocks and rolls". *News Physiol Sci 16*, 49-55.

(8) Trinick, J., and Tskhovrebova, L. (1999) Titin: a molecular control freak. *Trends Cell Biol 9*, 377-80.

(9) Gregorio, C. C., and Antin, P. B. (2000) To the heart of myofibril assembly. *Trends Cell Biol 10*, 355-62.

(10) Swynghedauw, B. (1986) Developmental and functional adaptation of contractile proteins in cardiac and skeletal muscles. *Physiol Rev 66*, 710-71.

(11) Clark, K. A., McElhinny, A. S., Beckerle, M. C., and Gregorio, C. C. (2002) Striated muscle cytoarchitecture: an intricate web of form and function. *Annu Rev Cell Dev Biol 18*, 637-706.

(12) Li, M. X., Wang, X., and Sykes, B. D. (2004) Structural based insights into the role of troponin in cardiac muscle pathophysiology. *J Muscle Res Cell Motil 25*, 559-79.

(13) Tripet, B., De Crescenzo, G., Grothe, S., O'Connor-McCourt, M., and Hodges, R. S. (2003) Kinetic analysis of the interactions between troponin C (TnC) and troponin I (TnI) binding peptides: evidence for separate binding sites for the 'structural' N-terminus and the 'regulatory' C-terminus of TnI on TnC. *J Mol Recognit 16*, 37-53.

(14) Gomes, A. V., Potter, J. D., and Szczesna-Cordary, D. (2002) The role of troponins in muscle contraction. *IUBMB Life 54*, 323-33.

(15) Tikunova, S. B., and Davis, J. P. (2004) Designing calcium-sensitizing mutations in the regulatory domain of cardiac troponin C. *J Biol Chem 279*, 35341-52.

(16) Gagne, S. M., Tsuda, S., Spyracopoulos, L., Kay, L. E., and Sykes, B. D. (1998) Backbone and methyl dynamics of the regulatory domain of troponin C: anisotropic rotational diffusion and contribution of conformational entropy to calcium affinity. *J Mol Biol 278*, 667-86.

(17) Zot, A. S., and Potter, J. D. (1987) Structural aspects of troponin-tropomyosin regulation of skeletal muscle contraction. *Annu Rev Biophys Biophys Chem 16*, 535-59.

(18) Farah, C. S., and Reinach, F. C. (1995) The troponin complex and regulation of muscle contraction. *Faseb J 9*, 755-67.

(19) Morimoto, S., and Ohtsuki, I. (1989) Ca^{2+} binding to skeletal muscle troponin C in skeletal and cardiac myofibrils. *J Biochem (Tokyo) 105*, 435-9.

(20) Morris, C. A., Tobacman, L. S., and Homsher, E. (2001) Modulation of contractile activation in skeletal muscle by a calcium-insensitive troponin C mutant. *J Biol Chem 276*, 20245-51.

(21) Morimoto, S., and Ohtsuki, I. (1994) Role of troponin C in determining the Ca^{2+}-sensitivity and cooperativity of the tension development in rabbit skeletal and cardiac muscles. *J Biochem (Tokyo) 115*, 144-6.

(22) Babu, A., Scordilis, S. P., Sonnenblick, E. H., and Gulati, J. (1987) The control of myocardial contraction with skeletal fast muscle troponin C. *J Biol Chem 262*, 5815-22.

(23) Lewit-Bentley, A., and Rety, S. (2000) EF-hand calcium-binding proteins. *Curr Opin Struct Biol 10*, 637-43.

(24) Krudy, G. A., Brito, R. M., Putkey, J. A., and Rosevear, P. R. (1992) Conformational changes in the metal-binding sites of cardiac troponin C induced by calcium binding. *Biochemistry 31*, 1595-602.

(25) Li, M. X., Spyracopoulos, L., and Sykes, B. D. (1999) Binding of cardiac troponin-I147-163 induces a structural opening in human cardiac troponin-C. *Biochemistry 38*, 8289-98.

(26) Gordon, A. M., Huxley, A. F., and Julian, F. J. (1966) The variation in isometric tension with sarcomere length in vertebrate muscle fibres. *J Physiol 184*, 170-92.

(27) Hofmann, P. A., and Fuchs, F. (1988) Bound calcium and force development in skinned cardiac muscle bundles: effect of sarcomere length. *J Mol Cell Cardiol 20*, 667-77.

(28) Akella, A. B., Su, H., Sonnenblick, E. H., Rao, V. G., and Gulati, J. (1997) The cardiac troponin C isoform and the length dependence of Ca^{2+} sensitivity of tension in myocardium. *J Mol Cell Cardiol 29*, 381-9.

(29) McDonald, K. S., Field, L. J., Parmacek, M. S., Soonpaa, M., Leiden, J. M., and Moss, R. L. (1995) Length dependence of Ca^{2+} sensitivity of tension in mouse cardiac myocytes expressing skeletal troponin C. *J Physiol 483 (Pt 1)*, 131-9.

(30) Gulati, J., Sonnenblick, E., and Babu, A. (1991) The role of troponin C in the length dependence of Ca^{2+}-sensitive force of mammalian skeletal and cardiac muscles. *J Physiol 441*, 305-24.

(31) Patel, J. R., McDonald, K. S., Wolff, M. R., and Moss, R. L. (1997) Ca^{2+} binding to troponin C in skinned skeletal muscle fibers assessed with caged Ca^{2+} and a Ca^{2+} fluorophore. Invariance of Ca^{2+} binding as a function of sarcomere length. *J Biol Chem 272*, 6018-27.

(32) Konhilas, J. P., Irving, T. C., and de Tombe, P. P. (2002) Myofilament calcium sensitivity in skinned rat cardiac trabeculae: role of interfilament spacing. *Circ Res 90*, 59-65.

(33) Dobesh, D. P., Konhilas, J. P., and de Tombe, P. P. (2002) Cooperative activation in cardiac muscle: impact of sarcomere length. *Am J Physiol Heart Circ Physiol 282*, H1055-62.

(34) Strauss, J. D., Van Eyk, J. E., Barth, Z., Kluwe, L., Wiesner, R. J., Maeda, K., and Ruegg, J. C. (1996) Recombinant troponin I substitution and calcium responsiveness in skinned cardiac muscle. *Pflugers Arch 431*, 853-62.

(35) Oliveira, D. C., and Reinach, F. C. (2003) The calcium-induced switch in the troponin complex probed by fluorescent mutants of troponin I. *Eur J Biochem 270*, 2937-44.

(36) Lehman, W., Rosol, M., Tobacman, L. S., and Craig, R. (2001) Troponin organization on relaxed and activated thin filaments revealed by electron microscopy and three-dimensional reconstruction. *J Mol Biol 307*, 739-44.

(37) Negele, J. C., Dotson, D. G., Liu, W., Sweeney, H. L., and Putkey, J. A. (1992) Mutation of the high affinity calcium binding sites in cardiac troponin C. *J Biol Chem 267*, 825-31.

(38) Golosinska, K., Pearlstone, J. R., Borgford, T., Oikawa, K., Kay, C. M., Carpenter, M. R., and Smillie, L. B. (1991) Determination of and corrections to sequences of turkey and chicken troponins-C. Effects of Thr-130 to Ile mutation on Ca^{2+} affinity. *J Biol Chem 266*, 15797-809.

(39) Layland, J., Solaro, R. J., and Shah, A. M. (2005) Regulation of cardiac contractile function by troponin I phosphorylation. *Cardiovasc Res 66*, 12-21.

(40) Endoh, M. (2002) Mechanisms of action of novel cardiotonic agents. *J Cardiovasc Pharmacol 40*, 323-38.

(41) Endoh, M. (2003) The therapeutic potential of novel cardiotonic agents. *Expert Opin Investig Drugs 12*, 735-50.

(42) Cleland, J. G., and McGowan, J. (2002) Levosimendan: a new era for inodilator therapy for heart failure? *Curr Opin Cardiol 17*, 257-65.

(43) Mathew, L., and Katz, S. D. (1998) Calcium sensitising agents in heart failure. *Drugs Aging 12*, 191-204.

(44) Arteaga, G. M., Kobayashi, T., and Solaro, R. J. (2002) Molecular actions of drugs that sensitize cardiac myofilaments to Ca^{2+}. *Ann Med 34*, 248-58.

(45) Gulati, J., Babu, A., and Su, H. (1992) Functional delineation of the Ca^{2+}-deficient EF-hand in cardiac muscle, with genetically engineered cardiac-skeletal chimeric troponin C. *J Biol Chem 267*, 25073-7.

(46) Blumenschein, T. M., Gillis, T. E., Tibbits, G. F., and Sykes, B. D. (2004) Effect of temperature on the structure of trout troponin C. *Biochemistry 43*, 4955-63.

(47) Gillis, T. E., Liang, B., Chung, F., and Tibbits, G. F. (2005) Increasing mammalian cardiomyocyte contractility with residues identified in trout troponin C. *Physiol Genomics*.

(48) Gillis, T. E., Blumenschein, T. M., Sykes, B. D., and Tibbits, G. F. (2003) Effect of temperature and the F27W mutation on the Ca^{2+} activated structural transition of trout cardiac troponin C. *Biochemistry 42*, 6418-26.

(49) Moreno-Gonzalez, A., Fredlund, J., and Regnier, M. (2005) Cardiac troponin C (TnC) and a site I skeletal TnC mutant alter Ca^{2+} versus crossbridge contribution to force in rabbit skeletal fibres. *J Physiol 562*, 873-84.

(50) Gulati, J., and Rao, V. G. (1994) The cardiac Ca^{2+}-deficient EF-hand governs the phenotype of the cardiac-skeletal TnC-chimera in solution by Sr^{2+}-induced tryptophan fluorescence emission. *Biochemistry 33*, 9052-6.

(51) Howarth, J. W., Krudy, G. A., Lin, X., Putkey, J. A., and Rosevear, P. R. (1995) An NMR and spin label study of the effects of binding calcium and troponin I inhibitory peptide to cardiac troponin C. *Protein Sci 4*, 671-80.

(52) Ngai, S. M., Sonnichsen, F. D., and Hodges, R. S. (1994) Photochemical cross-linking between native rabbit skeletal troponin C and benzoylbenzoyl-troponin I inhibitory peptide, residues 104-115. *J Biol Chem 269*, 2165-72.

(53) Smith, S. H., and Fuchs, F. (2000) Length-dependence of cross-bridge mediated activation of the cardiac thin filament. *J Mol Cell Cardiol 32*, 831-8.

(54) Valencia, F. F., Paulucci, A. A., Quaggio, R. B., Da Silva, A. C., Farah, C. S., and Reinach, F. C. (2003) Parallel measurement of Ca^{2+} binding and fluorescence emission upon Ca^{2+} titration of recombinant skeletal muscle troponin C. Measurement of sequential calcium binding to the regulatory sites. *J Biol Chem 278*, 11007-14.

(55) Farah, C. S., and Reinach, F. C. (1999) Regulatory properties of recombinant tropomyosins containing 5-hydroxytryptophan: Ca^{2+}-binding to troponin results in a conformational change in a region of tropomyosin outside the troponin binding site. *Biochemistry 38*, 10543-51.

(56) Schlesinger, S. (1968) The effect of amino acid analogues on alkaline phosphatase. Formation in Escherichia coli K-12. II. Replacement of tryptophan by azatryptophan and by tryptazan. *J Biol Chem 243*, 3877-83.

(57) Barlati, S., and Ciferri, O. (1970) Incorporation of 5-methyl- and 5-hydroxy-tryptophan into the protein of Bacillus subtilis. *J Bacteriol 101*, 166-72.

(58) Ludescher, R. D., Volwerk, J. J., de Haas, G. H., and Hudson, B. S. (1985) Complex photophysics of the single tryptophan of porcine pancreatic phospholipase A2, its zymogen, and an enzyme/micelle complex. *Biochemistry 24*, 7240-9.

(59) Wong, C. Y., and Eftink, M. R. (1998) Incorporation of tryptophan analogues into staphylococcal nuclease, its V66W mutant, and Delta 137-149 fragment: spectroscopic studies. *Biochemistry 37*, 8938-46.

(60) Moyes, C. D., Borgford, T., LeBlanc, L., and Tibbits, G. F. (1996) Cloning and expression of salmon cardiac troponin C: titration of the low-affinity Ca^{2+}-binding site using a tryptophan mutant. *Biochemistry 35*, 11756-62.

(61) Davis, J. P., Rall, J. A., Reiser, P. J., Smillie, L. B., and Tikunova, S. B. (2002) Engineering competitive magnesium binding into the first EF-hand of skeletal troponin C. *J Biol Chem 277*, 49716-26.

(62) Davis, J. P., Tikunova, S. B., Walsh, M. P., and Johnson, J. D. (1999) Characterizing the response of calcium signal transducers to generated calcium transients. *Biochemistry 38*, 4235-44.

(63) Dantzig, J. A., Goldman, Y. E., Millar, N. C., Lacktis, J., and Homsher, E. (1992) Reversal of the cross-bridge force-generating transition by photogeneration of phosphate in rabbit psoas muscle fibres. *J Physiol 451*, 247-78.

(64) Tikunova, S. B., Rall, J. A., and Davis, J. P. (2002) Effect of hydrophobic residue substitutions with glutamine on Ca^{2+} binding and exchange with the N-domain of troponin C. *Biochemistry 41*, 6697-705.

(65) Fitzsimons, D. P., and Moss, R. L. (1998) Strong binding of myosin modulates length-dependent Ca^{2+} activation of rat ventricular myocytes. *Circ Res 83*, 602-7.

(66) Gomes, A. V., and Potter, J. D. (2004) Molecular and cellular aspects of troponin cardiomyopathies. *Ann N Y Acad Sci 1015*, 214-24.

(67) Hoffmann, B., Schmidt-Traub, H., Perrot, A., Osterziel, K. J., and Gessner, R. (2001) First mutation in cardiac troponin C, L29Q, in a patient with hypertrophic cardiomyopathy. *Hum Mutat 17*, 524.

(68) Pearlstone, J. R., Chandra, M., Sorenson, M. M., and Smillie, L. B. (2000) Biological function and site II Ca^{2+}-induced opening of the regulatory domain of skeletal troponin C are impaired by invariant site I or II Glu mutations. *J Biol Chem 275*, 35106-15.

(69) Martyn, D. A., and Gordon, A. M. (2001) Influence of length on force and activation-dependent changes in troponin c structure in skinned cardiac and fast skeletal muscle. *Biophys J 80*, 2798-808.

(70) Regnier, M., Rivera, A. J., Wang, C. K., Bates, M. A., Chase, P. B., and Gordon, A. M. (2002) Thin filament near-neighbour regulatory unit interactions affect rabbit skeletal muscle steady-state force-Ca^{2+} relations. *J Physiol 540*, 485-97.

(71) Spyracopoulos, L., Li, M. X., Sia, S. K., Gagne, S. M., Chandra, M., Solaro, R. J., and Sykes, B. D. (1997) Calcium-induced structural transition in the regulatory domain of human cardiac troponin C. *Biochemistry 36*, 12138-46.

(72) Fujimori, K., Sorenson, M., Herzberg, O., Moult, J., and Reinach, F. C. (1990) Probing the calcium-induced conformational transition of troponin C with site-directed mutants. *Nature 345*, 182-4.

(73) Grabarek, Z., Tan, R. Y., Wang, J., Tao, T., and Gergely, J. (1990) Inhibition of mutant troponin C activity by an intra-domain disulphide bond. *Nature 345*, 132-5.

(74) Pearlstone, J. R., Borgford, T., Chandra, M., Oikawa, K., Kay, C. M., Herzberg, O., Moult, J., Herklotz, A., Reinach, F. C., and Smillie, L. B. (1992) Construction and characterization of a spectral probe mutant of troponin C: application to analyses of mutants with increased Ca^{2+} affinity. *Biochemistry 31*, 6545-53.

(75) Sia, S. K., Li, M. X., Spyracopoulos, L., Gagne, S. M., Liu, W., Putkey, J. A., and Sykes, B. D. (1997) Structure of cardiac muscle troponin C unexpectedly reveals a closed regulatory domain. *J Biol Chem 272*, 18216-21.

(76) Schmidtmann, A., Lindow, C., Villard, S., Heuser, A., Mugge, A., Gessner, R., Granier, C., and Jaquet, K. (2005) Cardiac troponin C-L29Q, related to hypertrophic cardiomyopathy, hinders the transduction of the protein kinase A dependent phosphorylation signal from cardiac troponin I to C. *Febs J 272*, 6087-97.

(77) D'Amico, S., Claverie, P., Collins, T., Georlette, D., Gratia, E., Hoyoux, A., Meuwis, M. A., Feller, G., and Gerday, C. (2002) Molecular basis of cold adaptation. *Philos Trans R Soc Lond B Biol Sci 357*, 917-25.

(78) Fields, P. A., and Somero, G. N. (1998) Hot spots in cold adaptation: localized increases in conformational flexibility in lactate dehydrogenase A4 orthologs of Antarctic notothenioid fishes. *Proc Natl Acad Sci U S A 95*, 11476-81.